Engineering Tumor Constructs to Elucidate the Impact of Microenvironment on Tumor Angiogenesis and Metastasis

by

Malak Nasser

A thesis submitted in partial fulfillment
of the requirements for the degree of
Master of Science in Engineering
(Bioengineering)
in the University of Michigan-Dearborn
2020

Master's Thesis Committee:

Associate Professor Gargi Ghosh, Chair
Professor Oleg Zikanov
Associate Professor Joe Fu-Jiou Lo

Acknowledgements

I would like to express my sincere appreciation to my advisor, Dr. Gargi Ghosh, for her encouragement and mentorship during the entirety of my research and the completion of my thesis. I also wish to thank Victoria Sears for her support and assistance as well as her friendship. Further, I wish to show my gratitude to Wu Yang and Swetaparna Mohanty for their laboratory training. I would also like to extend my appreciation to lab members Dina Shohatee, Youssef Danaoui, and Deepika Somayajula for their endless support. I also want to acknowledge Dr. Oleg Zikanov and Dr. Joe Lo for being part of the thesis defense committee. Additionally, I am thankful to the lab members of Dr. Lo, Dr. Kanapathipillai, and Dr. Argento for their friendship throughout my research. I am also indebted to my family and friends for their love, encouragement, and unwavering support. Moreover, I would like to thank the Alternatives Research and Development Foundation (AWD005747 and AWD007781) for their financial support. Finally, I am thankful to God for His countless blessings.

Table of Contents

List of Figures

List of Tables

List of Abbreviations

BSA	Bovine Serum Albumin
dECM	Decellularized Extracellular Matrix
DMEM	Dulbecco's Modified Eagle Medium
DMSO	Dimethylsulfoxide
DNA	Deoxyribonucleic Acid
DPBS	Dulbecco's Phosphate Buffered Saline
ECM	Extracellular Matrix
FBS	Fetal Bovine Serum
FITC	Fluorescein Isothiocyanate
GAGs	Glycosaminoglycans
HUVECs	Human Umbilical Vein Endothelial Cells
LIMK	LIM kinase
MLC	Myosin Light Chain
MMP	Matrix Metalloproteinases
MSCs	Mesenchymal Stem Cells
PDGF	Platelet Derived Growth Factor
PLG	Poly(lactide-co-glycolide)
PVA	Poly Vinyl Alcohol
RANKL	Receptor Activator of Nuclear Factor kappa-B Ligand
ROCK	Rho-associated Kinase
TCP	Tissue Culture Plate
uPA	Urokinase Plasminogen Activator
VEGF	Vascular Endothelial Growth Factor
5-FU	5-fluorouracil

Abstract

Breast cancer is the leading cause of cancer deaths among females globally. Although localized or early stage cancer is largely curable, the five-year survival rate significantly decreases after metastasis. The crosstalk between tumor microenvironment and neoplastic cells is the key for promoting tumor growth and stimulating tumor angiogenesis and metastasis to distant organs. In the first section of this study, the effect of stromal stiffening on the angiogenic activity of cancer cells was explored. Highly aggressive breast cancer cells, MDA-MB-231, displayed an increased expression of pro-angiogenesis-related signals when encapsulated in stiffer collagen matrices. In comparison, less-invasive cells, MCF-7, showed a minimal change in the release of angiogenic signals when cultured on stiffer matrices. Inhibition of mechanotransduction pathways on the angiogenic activity of aggressive tumor cells in stiff matrices was investigated using Y-27632, Blebbistatin, and Cytochalasin D. Rho associated kinase (ROCK) inhibitor, Y-27632, diminished the pro-angiogenic signal release, thereby suggesting the potential dependence of breast cancer cells on the Rho/ROCK pathway in regulating tumor angiogenesis.

Breast cancer cells most commonly metastasize to lungs, liver, and brain, with preferential metastasis to bone tissue. Initial stages of bone metastasis are not well understood, but studies suggest that the host microenvironment is manipulated into allowing the tumor cells to invade and proliferate at bone sites. In the second section of this study, the effect of microenvironment on bone metastasis was studied. Mesenchymal stem cells (MSCs) were differentiated into osteoblasts, and the deposited matrices were decellularized. The key components of the deposited extracellular matrix (ECM) were characterized. Furthermore, the effect of the decellularized ECM (dECM) on

the activity of breast cancer cells was investigated. In the presence of dECM, MDA-MB-231 cell proliferation increased, and the efficacy of anti-cancer drug, 5-fluorouracil, on the cancer cells was reduced.

Chapter 1: Introduction

More than 2,300 years ago, Hippocrates likened the long, enlarged veins protruding from breast tumors to the legs of a crab leading him to come up with the Greek term *karkinoma*, or the now more common Latin term, *cancer* [1]. It was not until after the work of Robert Hooke in the 1600s, with the discovery of the cell, and Rudolf Virchow in the 1800s, who recognized that diseases arose in the cells, that cancer would be understood as a disease of uncontrolled cell division [1]. Today, cancer is a term that refers to over 100 disease types; although similar in the general processes of the disease, each type is characterized by its own unique properties such as cause, location in the body, and invasiveness [1]. This study explores how the cellular environment affects the progression of tumors. To this end, it is important to understand how tumors develop by first understanding how cancerous cells are different from normal, healthy cells, how these differences arise, and what they entail in terms of cell behavior and disease.

A normal cell is restricted in its ability to grow and divide by specific genes that control a sequence of events, known as the cell cycle [1]. These genes can be categorized into two groups; one category referring to genes that promote cell division, known as proto-oncogenes, and another category that inhibits cell division, known as tumor suppressor genes [1]. In normal cells, these two categories regulate cell growth in an effort to maintain the size and structure of each tissue in the body. The balance in the expression of these two types of genes is dependent on several intra- and inter-cellular signals such as the concentration and type of growth factors present in the cell environment, as well as the cell-cell communication that results in contact inhibition [1]. Furthermore, normal cells are limited by the number of times they divide before they reach

senescence, a concept known as the Hayflick limit, after Leonard Hayflick, due to the shortening of the telomeres, or the ends of chromosomes, that occurs with each cell division [2].

Unlike normal cells, cancer cells have uncontrolled cell replication, which means that they have lost the restrictions that inhibit cell growth [1]. This loss is due to the mutations that occur in both the proto-oncogenes and the tumor suppressor genes. Mutated proto-oncogenes, or oncogenes, induce excessive cell growth by causing an increased expression of growth factors, by producing receptor proteins that release growth-promoting signals to the inside of the cell, or by disrupting the signaling pathway inside the cell such that the nucleus receives endless stimulatory signals[1, 3]. These mutations are responsible for the cancer cells' ability to grow despite the absence or reduced concentration of growth factors in their environment [1, 3]. Mutated tumor suppressor genes prevent the inhibition of cell division as they no longer prevent the flow of growth-related signals, or they no longer produce active proteins that are an integral part of certain inhibitory pathways within the cells. These mutations also provide cancerous cells with a key characteristic in which they do not exhibit contact inhibition, a process of halting cell division when cells come in contact with each other [1]. Additionally, mutations in other genes, such as DNA repair genes, prevent the cell's ability to repair DNA errors during replication, causing more frequent mutations than normal, some of which affect proto-oncogenes and tumor suppressor genes. Furthermore, cancer cells have the ability to divide indefinitely and, unlike normal cells, do not reach senescence due to the presence of the enzyme, telomerase, which replaces telomeric fragments that are clipped with each cell division [1, 3]. They also evade a key cellular defense mechanism known as apoptosis, in which diseased or injured cells undergo a programmed death [3]. The cell's ability to avoid this suicidal death, often through the inactivation of the p53 protein due to tumor suppressor gene mutations, contributes to the uncontrolled growth of tumor cells as

well as their resistance to chemotherapy or radiation treatment that would usually induce cell death by damaging the cell's DNA [1].

While the cause of these mutations has been linked to aging, exposure to carcinogens, and genetic susceptibility, current understanding of the development of cancer suggests that it is a multistep process that occurs over a long period of time [1]. The exact number of mutations required for a normal cell to transform into a cancerous one is not known. However, the stages of tumor development begin when enough mutations occur to disrupt the regulated growth of the cell [3]. The transformed cell and its daughter cells divide continuously, resulting in tissue enlargement or hyperplasia, an initial stage of cancer [3]. Eventually, one or a few of the dividing daughter cells might undergo another mutation, not only resulting in excessive division but also a different morphology, another stage of tumor development called dysplasia [3]. This phenomenon explains why although cancer cells within the same tumor type are monoclonal, individual cells may have different characteristics. A localized tumor that remains within the same tissue of origin is called *in situ* cancer and can remain within the same tissue for an indefinite period [1]. However, additional mutations that occur in some cells may cause the tumor to gain new abilities and characteristics, such as its ability to detach from the primary tumor and migrate to nearby tissues or distant organs if they gain access to the bloodstream [1]. In this case, the tumor becomes malignant and is called invasive cancer.

Regardless of the type of cancer, all solid tumors require an adequate supply of oxygen and nutrients and a means of byproduct or waste removal [4]. In fact, the ability of any tissue to grow beyond a certain size cannot merely rely on the passive diffusion of oxygen and nutrients due to the limitations it has on molecular transport over distance and time. The design of the cardiovascular system in the body ensures that there is enough blood flowing through the blood

vessels, or capillaries, that surround tissues and cells [5]. Tumors are no different than normal tissues in that regard. Tumor angiogenesis is the process by which blood vessels form and penetrate the cancer environment. This process is activated in response to hypoxia, where the cells in the tissue become oxygen deprived due to the high division rate of the tumor cells. When hypoxia is combined with a shortage of nutrients, the cells express various inflammatory signals that recruit vascular cells to form blood vessels at the tumor site [4]. Blood vessels are comprised of a monolayer of endothelial cells that form the inner lumen and stabilizing pericytes and vascular smooth muscle cells that form the exterior. Neovascularization, or the formation of new blood vessels, involves two mechanisms, vasculogenesis and sprouting angiogenesis [4]. Vasculogenesis is the formation of new blood vessels through the differentiation of vascular progenitor cells, while angiogenesis involves the formation of new blood vessels from preexisting blood vessels [6]. Of the two mechanisms, the latter is one of the most studied and understood process used by cancer cells to induce the formation of their own capillaries.

Sprouting angiogenesis begins with the destabilization of the basement lamina around endothelial cells, followed by the endothelial-mesenchymal conversion in which endothelial cells exhibit increased proliferation and migration from the original vessel into the connective tissue [7]. The new endothelial cells are connected to each other and to cells of the mother vessel through intercellular junctions so that the two lumens remain connected. Once the endothelial cells have formed an immature blood vessel, the process of vessel maturation begins. For this to occur, a reverse mesenchymal-endothelial conversion causes endothelial cells to return to their dormant state so that they do not continue to proliferate and migrate [8]. Furthermore, pericytes and vascular smooth muscle cells are recruited, and a new basement lamina is formed [8]. The steps involved in the development of these new blood vessels are guided by different stimuli from the tumor cells,

known as pro-angiogenic signals [4], resulting in a sustained angiogenic process that generates heavy vasculature to support the growing tumor, no different from the distended blood vessels of breast tumors that Hippocrates compared to crab limbs many centuries ago.

The selectivity for metastasis to specific sites is determined by the cancer cells' ability to complete the steps of the metastatic cascade. In order for metastasis to occur, cancer cells must first detach from the primary tumor, intravasate blood vessels, evade the immune system, and attach at new distant organs and proliferate resulting in the establishment of secondary tumors [9]. Certain metastatic cells prefer to grow in specific organs. In breast cancer, for example, metastasis affects the lungs, bones, liver, and brain, with bone being the preferred site [10]. Anatomical effects such as proximity and easy access to certain sites, as well as mechanical effects, such as blood flow, influence the location of metastasis [11]. However, it is the microenvironment that ultimately determines which metastatic site is favored and promotes tumor growth at that location. Tumor cells manipulate the host microenvironment by sending signals in the form of biochemical factors from the primary tumor site, adhering to endothelial cells at distant sites, and invading and colonizing the target site [12].

As a major component of tumor and host microenvironment, the extracellular matrix (ECM), a complex network of proteins and other macromolecules with specific biochemical and mechanical properties, plays an important role in tumor progression and metastasis [13-14]. The properties of the ECM determine the cell's ability to detect and respond to external stimuli, thereby regulating cell behavior and contributing to tumor progression [15]. The work in this thesis is divided into two sections. Part 1 will focus on investigating the effect of matrix stiffening on angiogenesis, while Part 2 will explore the role of the microenvironment in promoting secondary lesion formation.

SECTION I

MATRIX STIFFENING AND TUMOR ANGIOGENESIS

Chapter 2: Motivation and Objectives

Breast cancer is the most frequently diagnosed cancer and the leading cause of cancer death among females worldwide [16]. When diagnosed early or at a localized stage, the five-year survival rate increases to 98% as compared to a 27% survival rate after metastases [17]. When tumors begin to grow beyond 1-2 mm^3, the diffusion of nutrients and oxygen into the native tissue becomes insufficient to support the insatiable metabolic demands required for the continued growth and survival of the tumor cells [18]. Consequently, the cells release a combination of angiogenic factors to recruit endothelial cells from neighboring blood vessels and induce the formation of new blood capillaries, not only to provide the cells with the necessary oxygen and nourishment required for the cells' continued growth, but also to provide an avenue through which these cells can migrate and reach distant organs in the body [19]. Therefore, angiogenesis, i.e. the formation of blood vessels from pre-existing vessels, becomes the rate-limiting step for tumors to grow and metastasize [20]. Specifically, a change in the balance between regulatory pro- and anti-angiogenic factors, leading to the increase in the net stimulatory activity and the onset of angiogenesis, triggers metastatic tumor growth [21].

Recent inquiries into tumor progression allude to the importance of microenvironmental biophysical cues in stimulating the aggressive phenotype of cancer cells [13-14]. As a major component of tumor microenvironment, extracellular matrix (ECM) is believed to play an important role in tumor development and metastasis [13-14]. The ECM is a complex network consisting of distinct macromolecules which result in a matrix with specific physical, biochemical, and mechanical properties [22]. Together, these properties provide the structural support for the

cellular components of tissues and pertain to the signaling mechanisms that determine the cell's ability to sense and react to external mechanical forces, thereby actively regulating cell behavior and contributing to tumor progression [15, 22, 23, 24]. Type I and IV collagen proteins are the most prevalent components of the ECM providing the main structural support for the interstitial matrix and the key component of the basement membrane, respectively [25-27]. Typically, tumor tissue is stiffer than healthy tissue owing to the continuous remodeling of the ECM, due to elevated production, deposition, and altered organization of collagen and related macromolecules, in tandem with increased metalloproteinase (MMP) activity [24]. Cancer cells recognize the increase in matrix stiffness and respond by generating increased traction forces on their surroundings through actomyosin and cytoskeleton contractility [28]. This increased stiffness leads to a series of signaling cascades that regulate gene expression and result in enhanced cancer cell growth and migration and contribute to the invasive phenotype, commonly associated with tumors [29].

However, despite the importance of tumor stroma stiffening and the centrality of vascularization in tumor progression, how the mechanical forces are co-opted in the cancer cell signal transduction pathways, and, ultimately, in the angiogenic response of the cancer cells remains unclear. We demonstrated in our previous studies, using mechanically tuned hydrogels, that the matrix stiffening of the highly aggressive breast cancer cell line, MDA-MB-231, not only promotes cell proliferation and migration, but it also correlates with higher levels of VEGF expression, indicating stimulated angiogenic activity by the cells [30]. Furthermore, inhibition of actomyosin organization reduced VEGF secretion by the cancer cells [30]. Another recent study has reported upregulated VEGF expression by hepatocellular carcinoma (HCC) cells when cultured on stiffer matrices [31]. Together, these studies suggest the potential existence of a regulatory mechanotransduction pathway that may govern the angiogenic activity of tumor cells.

We hypothesize that ECM stiffening during tumor progression regulates the pro-angiogenic signaling of cancer cells and interruptions in the mechanotransductive pathway may have a therapeutic potential in disrupting vascularization and slowing tumor progression. Therefore, this work is aimed at understanding how changes in the mechanical properties of tumor microenvironment influence the angiogenesis signaling by cancer cells. The research conducted in this study addressed the following four objectives, which will be explored more deeply in the upcoming chapters.

Objective 1: Develop and characterize 3D scaffolds of varying stiffness. Three dimensional scaffolds with different compliances were fabricated from collagen protein and characterized for their stability, swelling, microstructures, and macromolecular diffusion.

Objective 2: Explore the effect of matrix stiffness on signaling profile of aggressive breast cancer cells. MDA-MB-231 cells were encapsulated in the gels of varying stiffness. Their proliferation, morphology, and the release of angiogenic factors as a function of matrix mechanics was examined. The bioactivity of the released biomolecules was also assessed through the proliferation activity of human umbilical vein endothelial cells (HUVECs).

Objective 3: Explore the effect of matrix stiffness on the signaling profile of non-aggressive breast cancer cells. MCF-7 cells were encapsulated in the gels of varying stiffness. Their proliferation, morphology, and the release of angiogenic factors was studied.

Objective 4: Test the effect of mechanotransduction inhibitors on the angiogenic activity of cancer cells. Inhibitors targeting the mechanotransduction pathway were added to aggressive breast cancer cells encapsulated in stiff matrices. Their effect on the signals released by the cells was studied.

Chapter 3: Fabrication and Characterization of Collagen Hydrogels

Introduction

Hydrogels are three dimensional networks of crosslinked hydrophilic polymer chains, named for their ability to retain significant amounts of water. This ability to absorb water, along with their other characteristics, such as biocompatibility, porosity, and tunable mechanical strength and biodegradability suggests their potential applications in tissue engineering [32]. Hydrogels can be fabricated from either natural or synthetic polymers. Synthetic polymers are usually chosen over natural hydrogels due to their longer service life, higher capacity of water absorption, and a greater mechanical strength [32]. Nonetheless, hydrogels made from naturally derived polymers are sometimes preferred in certain applications due to their composition and fiber organization that contributes to their ability to more closely mimic the extracellular matrix (ECM) [33].

Hydrogels made from collagen are one of the most popular and have been used to study "soft" tissues such as the skin, cartilage, and vascular structures [34]. The preference of collagen in tissue engineering application arises from it being one of the major components of the ECM [33]. However, applications of collagen hydrogels are limited due to their high compliance and low ability to retain their shape. To solve this problem, collagen gels are processed by the addition of various crosslinkers and exposure to different treatments that increase the mechanical strength of the scaffolds while simultaneously making them cytotoxic or inappropriate for cross linking in the presence of cells [34]. For this reason, other methods have been developed to promote collagen crosslinking and increase mechanical strength, thereof. One such method is non-enzymatic

glycation of collagen with reducing sugars, such as ribose or glucose, which allows cross-linking of cell-seeded collagen structures [34].

Non-enzymatic glycation is carried out through the Maillard reaction, where the aldehyde group on reducing sugars reacts with amino groups on collagen. The reaction produces a Schiff base which forms Amadori products that eventually form glycation end products. The accumulation of these end products in tissues results in a change in their mechanical and biochemical properties, as observed in conditions such as aging and diabetes [34]. Due to the ability to achieve this change in mechanical properties, a non-enzymatic pre-glycation approach was used to fabricate collagen gels of varying stiffness.

To ensure that these mechanically tuned hydrogels were stable and would retain their shape, the rate of degradation was measured. Furthermore, the degree of swelling was also studied, and their internal microstructure was examined. Since the goal of this study is to understand how cell angiogenic activity is affected in environments of different stiffness, it was important to ensure that the collagen gels would allow the diffusion of nutrients and oxygen molecules into the gel and waste products and released signals out of the gel to be profiled. For this reason, the diffusion kinetics of the collagen constructs were considered.

Methods

Fabrication of Collagen Gels

To fabricate mechanically tunable gels without altering the protein concentration, non-enzymatic pre-glycation of collagen, known as Maillard reaction, was carried out as described earlier [34]. Briefly, rat tail high concentration collagen type I solutions (Corning, MA) were mixed with 500 mM ribose (Thermofisher Scientific, MA) to form glycated collagen solutions with a final concentration of 0, 50, 100, 200, and 250 mM ribose in 0.02N acetic acid (Fisher Chemical, NJ) and incubated for 5 days at 4°C [34]. Following pre-glycation, collagen gels were

fabricated according to the manufacturer's protocol. Briefly, glycated collagen solutions were neutralized with 1M sodium hydroxide (NaOH, Sigma Aldrich, MO) in 10X Dulbecco's Phosphate Buffer Saline (DPBS, Gibco, NY) and diluted with distilled water. Collagen gels were formed by adding 250 µL of the neutralized solution to the wells of a 48-well plate and allowed to cross-link for 30 minutes in an incubator at 37°C to form gels with a final collagen concentration of 1.5 mg/mL.

Degradation

To measure the rate of collagen gel degradation, the samples were incubated in 2.5 units/mL collagenase type I (Gibco, NY) solution on a rotator shaker at room temperature. The weights of the gels were measured each day for 10 days, consecutively. The degradation ratio was calculated by normalizing the weights of the samples at each day to the weights of the samples on the day of fabrication.

Swelling Ratio

To measure the swelling ratio (Q_m) of the collagen gels, the samples were incubated in DPBS for 72 hours on a rotator shaker at room temperature following gel formation. The wet weights of the hydrated gels were measured. The hydrogels were then dried at 37°C overnight, and their dry weights were measured. The swelling ratio of the hydrogels was then calculated as a ratio of wet weights to dry weights.

Diffusion

To measure the rate of diffusion of macromolecules from the gels, fluorescein isothiocyanate-dextran (FITC-dextran) molecules of 150K MW (Sigma Aldrich, MO) were added to the neutralized collagen gel solution at a concentration of 50 µg/mL (w/v), and the collagen gels were fabricated after incubation for 30 min at 37°C. The gels were washed and incubated in DPBS

for seven days. Each day, the buffer solution containing the diffused molecules was collected and replaced with 500 µL of fresh DPBS. The fluorescence intensity for each sample was measured using SpectraMax M3 Multi-Mode Microplate Reader at excitation/emission wavelengths 495/519 nm. The diffusive release was calculated as a percentage using the following equation:

$$Release\ (\%) = 100 \times \frac{Amount\ of\ dextran\ molecules\ released\ each\ day\ (g)}{Amount\ of\ dextran\ molecules\ in\ the\ gel\ after\ wash\ (g)}$$

To determine the mechanism of macromolecule release through the collagen gels, the following Korsmeyer-Peppas equation was used:

$$F = \frac{M_t}{M_0} = kt^n$$

where F is the fractional release of the molecule, M_t is the amount of dextran diffused at any time, M_0 is the total initial amount of dextran that was encapsulated within the gels, k is the kinetic constant, t is time, and n is the diffusional exponent. Where $n \leq 0.5$, the transport of macromolecules can be defined by Fick's diffusion alone. Where $0.5 > n \leq 0.9$, the transport of molecules is governed by both diffusion and polymer relaxation/erosion, and for $n > 0.9$, polymer relaxation/erosion define the release of molecules. The data fitting was carried out for $\frac{M_t}{M_0} = 60\%$. At least three independent experiments were performed with five replicates per experiment.

Scanning Electron Microscope

Collagen gels were fabricated and left to dry overnight at 50℃. The dried samples were subjected to gold sputtering for 7 seconds. Images of the collagen fibers and pores were then captured using Zeiss scanning electron microscope (LEO 1455 VP).

Results and Discussion

The mechanical properties of the collagen hydrogels were altered via non-enzymatic pre-glycation in which the concentration of ribose was varied from 0 mM to 250 mM, while the

concentration of collagen was kept constant at 1.5 mg/mL. Mason and coworkers showed that an increase in ribose concentration resulted in an increase in mechanical stiffness of the hydrogels as demonstrated by a fourfold increase in compressive modulus from approximately 175 Pa to 730 Pa [35]. In this study, the integrity of the collagen gels was assessed by measuring enzymatic degradation profiles in the presence of collagenase. Over the 10-day period, a decrease in the normalized weights of the gels was observed, irrespective of ribose treatment (Fig 1). This decrease in weights corresponded to their degradation in presence of collagenase. All the gels retained their physical integrity over the course of the 10 days, indicating no effect of pre-glycation on the degradation of the gels (p-value > 0.05). Since, the goal of this study is to investigate the effect of matrix stiffness on cancer cell behavior, the collagen gels with the lowest and highest compression moduli were selected for further studies.

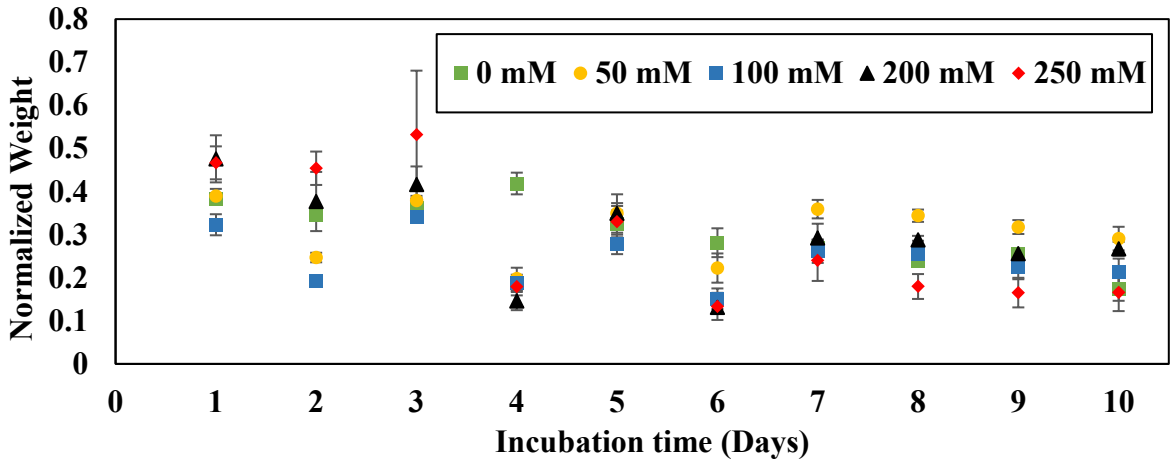

Figure 1. Degradation of pre-glycated (0 mM, 50 mM, 100 mM, 200 mM, and 250 mM ribose) collagen gels monitored over 10 days. Error bar S.E.M (N=3).

The effect of pre-glycation treatment on the swelling ratio of the collagen gels was also investigated. As shown in Table 1, the swelling ratio of the gels decreased from 73.8 ± 10.9 (collagen gels without ribose treatment) to 49.6 ± 6.5 (collagen treated with 250 mM ribose). In addition, the internal microstructure of the collagen gels was also studied using scanning electron

microscopy. The ribose treatment and the consequent change in mechanical properties did not alter the organization of collagen fiber structures (Fig 2).

Table 1. Comparison of swelling ratio and diffusional exponent of hydrogels as a function of ribose concentration

Ribose Concentration	Swelling Ratio	Diffusion Exponent
0 mM	73.7513 ± 10.8857	0.567838 ± 0.030944
250 mM	49.5730 ± 6.4934	0.627931 ± 0.008974

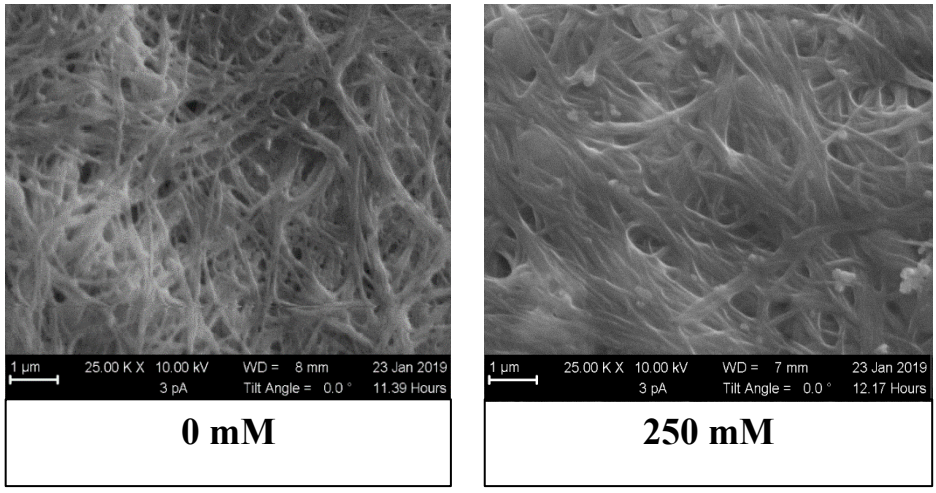

Figure 2. Scanning electron microscope images of collagen network.

To assess whether non-enzymatic pre-glycation altered the free volume available for transport of macromolecules across the hydrogels, the macromolecular release kinetics was investigated. For this purpose, collagen disks (with or without incubation with 250 mM ribose) were fabricated encapsulating FITC-conjugated (150kDa) dextran. Figure 3 compares the cumulative release (% released) of dextran over a span of 7 days. No significant difference in release kinetics of macromolecules from the collagen gels was observed as a function of ribose treatment. To investigate the release mechanism, the fractional release data was fitted into Korsemeyer-Peppas equation and the fitting parameters were calculated. The average values of

diffusional exponent (n) for the collagen gels were found to be greater than 0.5, but less than 0.9 (Table 1), thereby suggesting that the transport of macromolecules across the gels is via, both, Fickian diffusion as well as polymer relaxation/erosion.

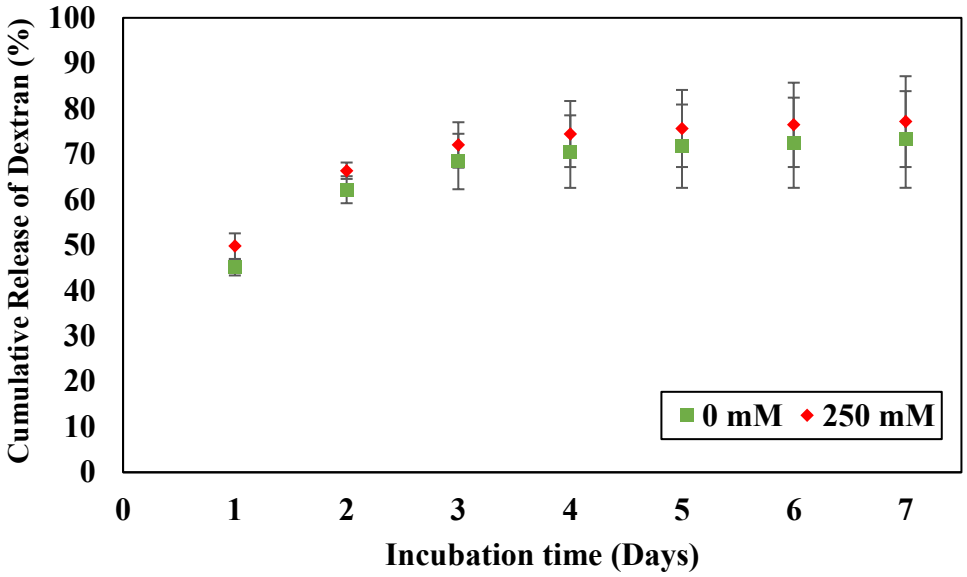

Figure 3. Percentage of cumulative dextran released from collagen gels (0 mM and 250 mM) over 7 days. Error bar S.E.M (N=3).

Chapter 4: Effect of Matrix Stiffness on Aggressive Breast Cancer Cell Behavior

Introduction

The stroma of cancerous breast tissue becomes 5-20 times stiffer than that of normal breast tissue [36]. This stiffness is due to a change in the tumor microenvironment through an increased deposition of collagen and/or its reorganization. This change in the structure and, ultimately, the properties of the ECM affects mammary epithelial cell shape, enhances cell growth, encourages cell invasion, and, overall, contributes to tumor development [24]. Recent studies have highlighted the role of the ECM and its components on tumor vascularization, a necessary and key characteristic of tumor cells. One such example involves integrin clustering, a key transmembrane protein that allows cell-ECM adhesion, which was shown to upregulate the expression of vascular endothelial growth factor (VEGF) by cancer cells, an important promoter of angiogenesis [37].

Although it is already established that the increased stiffness has a major effect on the behavior of cancer cells, not much is understood about how this change in stiffness affects tumor angiogenesis, especially in malignant cancers. A previous study found that aggressive breast cancer cells, not only exhibited an increase in proliferation and motility when seeded on rigid matrices, but also stimulated the expression of VEGF [30]. This suggests that the increased rigidity of the tumor microenvironment plays a regulatory role in angiogenic signaling of cancer cells. Here, the impact of stiffness on the angiogenesis release by malignant tumor cells is explored in depth by analyzing the secretion levels of pro- and anti-angiogenic factors released into the medium by the cells. For this purpose, MDA-MB-231 cells, which were isolated and expanded from a patient with invasive ductal carcinoma, were used. The cells were encapsulated in collagen

hydrogels, and their angiogenic signaling was profiled using a human angiogenesis antibody assay. Furthermore, the bioactivity of the released signals was studied by testing the proliferation of human umbilical vein endothelial cells (HUVECs).

Methods

Cell Culture

Highly invasive breast cancer cells (MDA-MB-231) and low invasive breast cancer cells (MCF-7) were purchased from American Type Culture Collection (ATCC) and expanded in RPMI 1640 Medium and Dulbecco's Modified Eagle Medium (DMEM), respectively; each supplemented with 10% (v/v) fetal bovine serum (FBS) and 1% (v/v) penicillin-streptomycin. Human umbilical vein endothelial cells (HUVECs) were obtained from (ATCC) and expanded in endothelial cell nasal medium-2 (EBM-2) supplemented with 1% (v/v) penicillin-streptomycin and EGM-2 Single Quots (containing FBS, hydrocortisone, hFGF, VEGF, R3-IGF-1, ascorbic acid, hEGF, GA-100, and heparin). Cells were cultured and incubated at 37℃ and 5% CO_2. In this study, MDA-MB-231 cells were used up to passage 7. HUVECs were used up to passage 6.

Cell Proliferation

Following detachment from the flasks using 0.25% Trypsin-EDTA, resuspended MDA-MB-231 cells were incorporated into the collagen gels by adding the cells to neutralized collagen solutions at a density of 12.5 x 10^4 cells/gel and incubated in 300 μL of serum-free media at 37 ℃ and 5% CO_2 after gel formation. Collagen gels were collected and frozen immediately after gels were formed, and again after 2, 4, and 6 days. The collected samples were digested with papain solution at 37 ℃ for 3 hours. The papain solution was created by dissolving 0.1M sodium acetate, 0.01M Na_2EDTA, and 0.005M cysteine hydrochloride in 0.2M sodium phosphate buffer and adding papain suspension (Sigma-Aldrich, MO). Cell proliferation was assessed using Quant-iT™ dsDNA High-Sensitivity Assay Kit (Thermo Fisher, USA). The fluorescence intensity was then

measured using SpectraMax M3 Multi-Mode Microplate Reader at excitation/emission wavelengths 480/530 nm. Cell proliferation over time was calculated as a percentage by dividing the fluorescence intensity of the gels at each day over the day of fabrication using the following equation:

$$Normalized\ Cell\ Growth\ (\%) = 100 \times \frac{RFU_{Any\ Day}}{RFU_{Day\ 0}}$$

The data was collected from at least three-independent experiments, each of which was carried out in three replicates.

Immunostaining

MDA-MB-231 cells incorporated into collagen gels at a cell density of 2.5 x 10^4 cells/gel were stained with 1% (v/v) Hoechst 33342 dye for 5 min. The cells were then fixed and permeabilized with 1:1 acetone:methanol solution at -20°C for 20 min. The cells were then blocked with 5% (w/v) BSA solution for 1 h, washed with 1X DPBS three times, and incubated with 2.5% (v/v) Alexa Fluor 488-phalloidin antibody for 1 h at 37°C. Following which, the cells were washed three times with 1X DPBS, and images were captured using Olympus laser scanning confocal microscope (FV 1200) to visualize the actin arrangement of the cell.

Quantification of Released Angiogenic-related Factors

To quantify the release of angiogenic factors by highly aggressive breast cancer cells as a function of microenvironment, MDA-MB-231 cells were encapsulated within collagen gels at a density of 12.5 x 10^4 cells/gel in 48 well plates and incubated in serum-free media. Four days post-fabrication, the spent media was collected and concentrated using Vivaspin 2 (2000 MWCO) centrifugal concentrators. Angiogenic molecules in the media were measured via Proteome Profiler™ Human Angiogenesis Array from R&D Systems. Bio-Rad Molecular Imager with ChemiDoc XRS+ Imaging System was used to image the membranes, and the average intensity of

each angiogenic factor was measured using the Image Lab Software (Version 4.1). The angiogenesis array was run two times.

Proliferation of HUVECs

HUVECs were seeded in 96 well at a density of 1 x 10^4 cells/well and incubated in the presence of concentrated media (collected from encapsulated cancer cells after 4 days) containing released angiogenic factors at 37℃ and 5% CO_2. Cells incubated in endothelial cell growth media and serum-free RPMI media served as the positive and negative controls, respectively. After 48 h of incubation, AlamarBlue cell viability reagent was added to fresh media and allowed to incubate for 3.5 h at 37℃ and 5% CO_2 and the fluorescence intensity was then measured using SpectraMax M3 Multi-Mode Microplate Reader at excitation/emission wavelengths 570/595 nm. Cell growth was then calculated as a percentage using the equation below:

$$Normalized\ Cell\ Growth\ (\%) = 100\ x\ \frac{(RFU_{sample} - RFU_{blank})}{RFU_{control}}$$

The data was collected from at least three independent experiments with three replicates per experiment.

Results

To study the impact of ECM stiffening on cellular behavior, highly invasive breast cancer cells (MDA-MB-231) were encapsulated within collagen gels of varying stiffness. Towards this goal, 5 x 10^4 cells/mL were suspended within collagen solution. 250 μL of the solution was then added in the wells of 48-wellplates and incubated at 37℃ and 5% CO_2 for 30 minutes. DNA quantification was used to assess the cell viability of the cells 2, 4, and 6 days post encapsulation. When MDA-MB-231 cells were encapsulated within the compliant gels (Fig 4), a significant increase in cell growth was observed compared to day 0 (p-value < 0.05). Moreover, it was

observed that beyond day 4, the increase in cell growth was not statistically different (p-value > 0.05). On the other hand, when encapsulated within the stiffer collagen gels, a subtle increase in growth of MDA-MB-231 cells was observed on day 2 compared to day 0 (p-value < 0.05). When cultured for longer period of time, no difference in cell growth was observed compared to day 2 (p-value > 0.05).

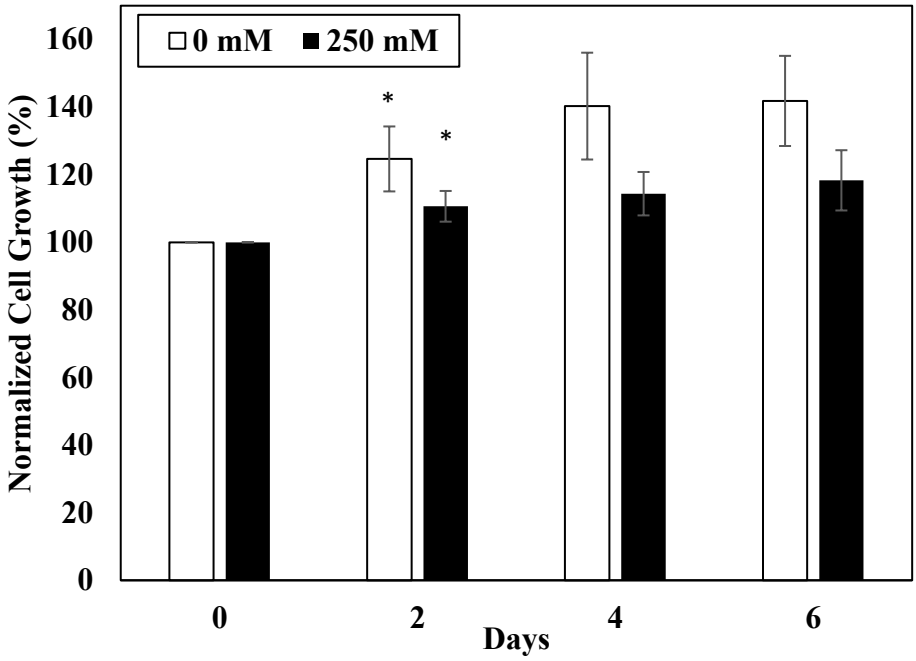

Figure 4. Proliferation of MDA-MB-231 cells encapsulated in glycated (250 mM) and non-glycated (0 mM) gels. Cell growth was assessed after 2, 4, and 6 days and compared to the day of fabrication. Error bar S.E.M (N=3). (*p-value<0.05 in comparison to day 0).

Four days post-fabrication, the F-actin cytoskeleton of the cells was stained by Alexa Fluor 488 conjugated phalloidin antibody and the confocal images of the cells were captured. As demonstrated in Fig 5, while MDA-MB-231 cells displayed stress fiber formation irrespective of matrix stiffness; however, manifestation of invadopodia, actin-based protrusion of the plasma membrane, was observed primarily in the ribose treated collagen gels.

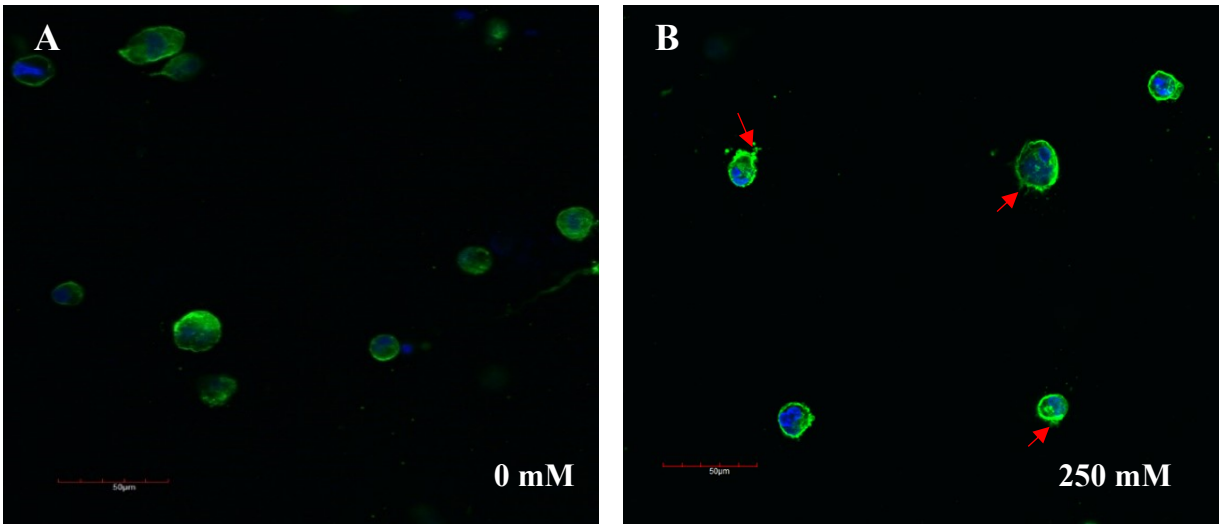

Figure 5. The confocal images of MDA-MB-231 cells in (A) soft and (B) stiff collagen gels displaying the arrangement of actin fibers (green). Hoechst 33342 (blue) stained the nuclei of the cells. The scale bar corresponds to 50 μm.

To investigate how matrix mechanics influences the release of angiogenic factors by the cancer cells, four days post-fabrication, the serum-free conditioned media was collected, and the angiogenic molecules were measured via Proteome Profiler Human Angiogenesis. The release of pro-angiogenic molecules by MDA-MB-231 cells encapsulated within collagen gels treated with 250 mM ribose (730 Pa) was compared with those encapsulated with collagen gels without treatment with ribose (0 mM, 175 Pa) (Fig 6A). As observed, stiffer gels stimulated angiogenic signaling of the cancer cells as manifested from enhanced secretion of pro-angiogenesis related factors. In addition, multiple pro-angiogenesis factors including angiogenin, angiopoietin-1, CXCL16, EGF, EG-VEGF, endoglin, FGF acidic, FGF basic, FGF-4, FGF-7, HGF, leptin, MCP-1, MMP-8, PDGF-AA, PDGF-AB/PDGF-BB, PIGF, VEGF-C were released only when the cells were encapsulated within stiffer gels. On the other hand, comparison of secretion of anti-angiogenic molecules revealed no drastic difference in the secretory signatures of cancer cells when matrix stiffness was altered (Fig 6B). Few anti-angiogenesis factors including ADAMTS-1, angiostatin/plasminogen, endostatin/collagen XVIII, platelet factor 4, serpin B5, and vasoinhibin

were released only by cells encapsulated within the stiffer gels, albeit the expression level was very low.

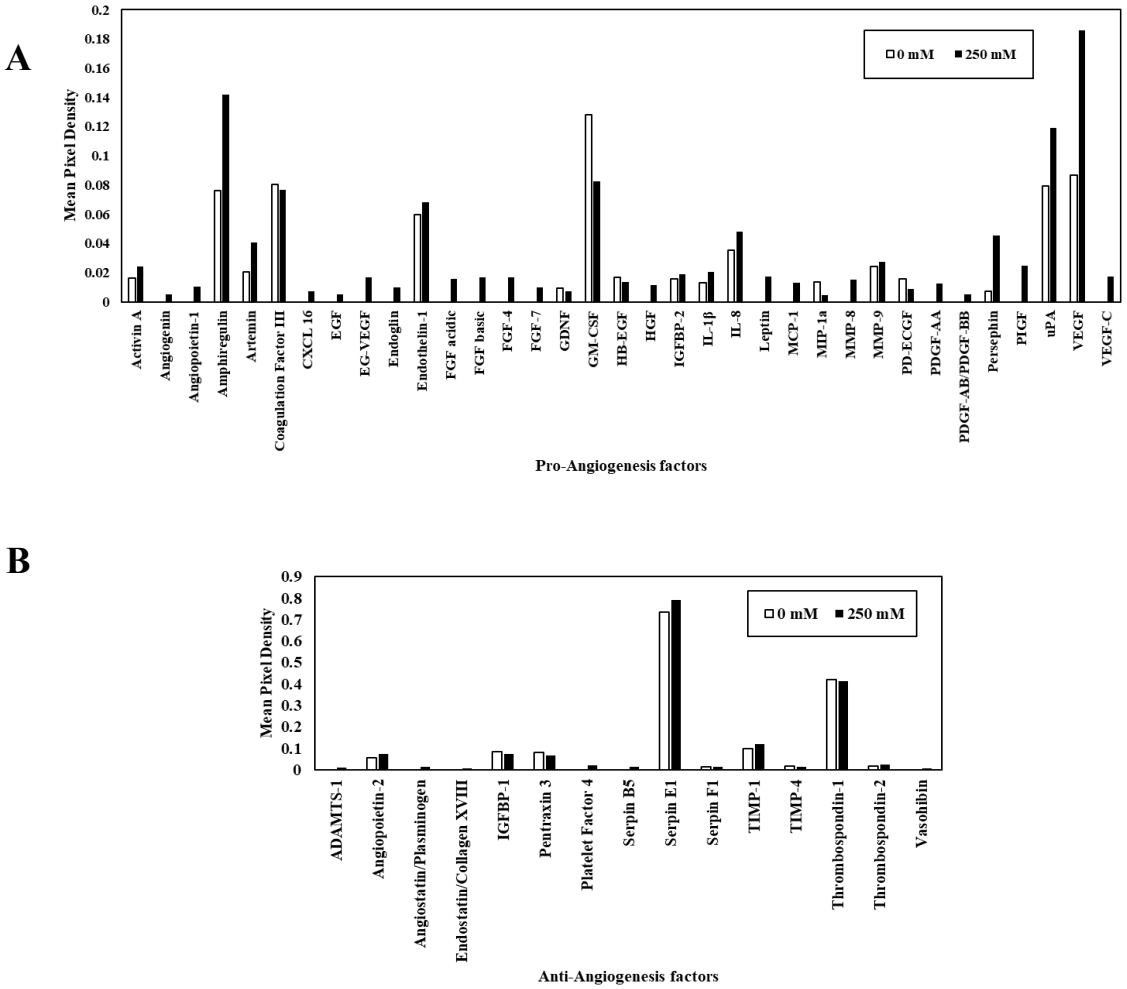

Figure 6. Effect of matrix stiffness on angiogenic activity of MDA-MB-231 cells. The mean pixel density of (A) pro-angiogenic factors and (B) anti-angiogenic factors released by MDA-MB-231 cells encapsulated in compliant (0 mM) and stiff (250 mM) collagen gels assayed via Angiogenesis Proteome Profiler.

Further, for quantitative analysis of angiogenic signaling of MDA-MB-231 cells, the signal intensities of the pro-angiogenic factors released by the cells encapsulated within stiffer gels were normalized with respect to the compliant gels. The expression levels of multiple pro-angiogenic molecules including activin A, amphiregulin, artemin, IL-1β, persephin, uPA, and VEGF were upregulated (normalized values > 1.5) (Fig 7A) whereas the expression levels of anti-angiogenic molecules remained unchanged (0.5 < normalized values < 1.5) (Fig 7B).

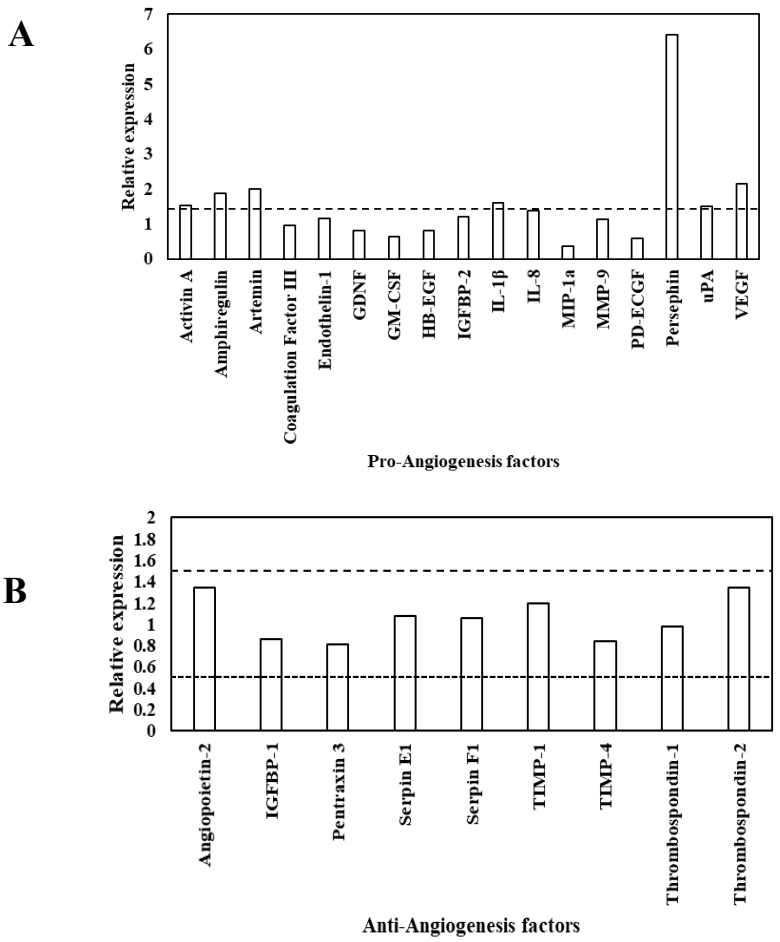

Figure 7. The normalized expression of angiogenesis related factors released by MDA-MB-231 encapsulated within glycated gels with respect to those released from non-glycated gels. The normalized expression of (A) pro-angiogenic factors and (B) anti-angiogenic factors. The closely dashed and widely dashed lines corresponds to the relative expression of 0.5 and 1.5, respectively.

To study the effect of this angiogenic cocktail on the proliferation of endothelial cells, conditioned media was collected 4 days post-encapsulation of MDA-MB-231 cells within collagen gels. HUVECs were seeded at a density of 1 x 10^4 cells/well in 96 well plates in the presence of conditioned media, and their cell growth was assessed. HUVECs cultured in presence of supplemented endothelial cell growth media and serum-free RPMI media acted as the positive and negative controls, respectively. To quantitatively assess the effect of conditioned media on growth of HUVECs, proliferation of cells was normalized with respect to cells incubated in supplemented endothelial cell media. Figure 8 shows an increase in growth of endothelial cells in the presence

of conditioned media collected from MDA-MB-231 cells incubated in the stiffer gel. However, the increase in growth was insignificant (p-value > 0.05).

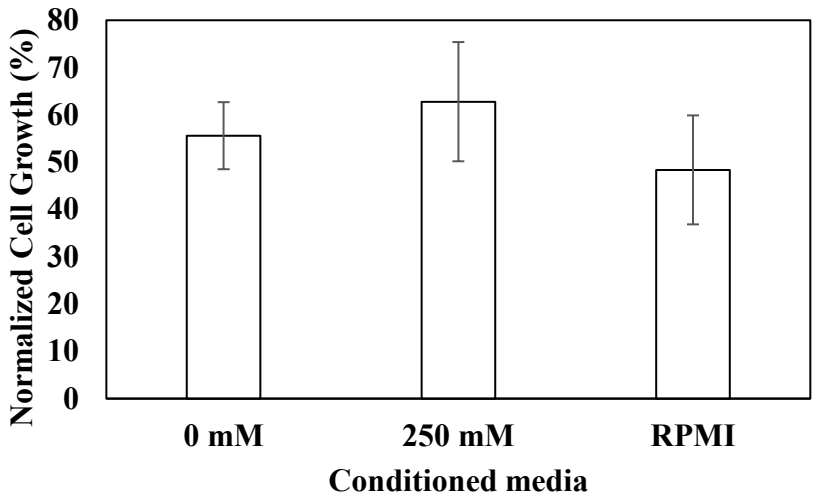

Figure 8. Effect of released angiogenic factors on the proliferation of HUVECs. Cell growth in the presence of conditioned media collected at Day 4 was normalized with respect to that in presence of HUVECs media (control). Error bar S.E.M (N=3).

Discussion

Recent studies attempting to better understand the factors influencing tumor progression have drawn attention to components of the tumor microenvironment, specifically the ECM. The continuous remodeling of the ECM contributes to a stiffer matrix in tumor tissue, thereby activating signaling pathways that stimulate tumor progression through increased cell proliferation and migration [29]. However, little is known about how this increased stiffness affects the signaling pathways that control the angiogenic activity of cancer cells. Breast tissue, considered a soft tissue under physiological conditions, stiffens markedly with tumor development leading to alteration in the micro-environmental physical forces [38-39]. In this current study, we sought to understand how this matrix stiffening alters the pro-angiogenic activity of cancer cells. Towards this goal, we developed 3D scaffolds of varying compliances (175 kPa and 730 kPa) using a non-enzymatic pre-glycation approach. The highly aggressive breast cancer cells (MDA-MB-231)

were encapsulated in the collagen gels, and the angiogenesis-related factors secreted by the cells were profiled. The increase in stiffness translated to the expression of multiple pro-angiogenic factors that were not expressed by the cells encapsulated in the compliant gels (angiogenin, angiopoietin-1, FGF acidic, basic, FGF-4, and FGF-7, PDGF, CXCL16, EGF, EG-VEGF, Endoglin, HGF, Leptin, MCP-1, MMP-8, PDGF-AA, PIGF, VEGF-C) along with an upregulation of several pro-angiogenic factors that were expressed in both including activin A, amphiregulin, artemin, IL-1β, persephin, uPA, and VEGF. This is consistent with previous studies where MDA-MB-231 were found to express higher levels of VEGF when seeded on matrices of increased stiffness [30]. In tumors, VEGF is secreted by cancer cells and surrounding stroma and contributes to tumor progression and invasion, increased blood vessel density, and metastasis [40, 41]. Moreover, VEGF and PDGF both play a role in inducing intussusceptive angiogenesis, a process found in many cancers including breast cancer [40, 42-43]. The upregulation of MMP (matrix metalloproteinase) and uPA (urokinase plasminogen activator) in the stiffer matrices is of key significance as it has been shown to modulate VEGF-mediated cell invasion by degrading the basal membrane and extracellular matrix and allowing endothelial cells to migrate and form sprouts [40, 44, 45]. FGF has been shown to not only play a role in tumor angiogenesis, but also have a role in initiation or promotion of tumorigenesis [46]. Angiogenin, which was only expressed by cells in the stiffer matrix promotes tumoral growth and angiogenesis [47], and angiopoietin-1 stimulates vessel maturation and their stabilization [40]. Leptin, the hunger-inhibiting hormone, was also expressed only by the cells encapsulated in the stiffer matrix, and studies have highlighted its role in breast carcinogenesis as it affects ER signaling and aromatase activity [48-50].

Chapter 5: Effect of Matrix Stiffness on Non-Aggressive Breast Cancer Cell Activity

Introduction

It has been established in earlier chapters that the ECM in tumor microenvironments plays an important role in regulating cancer cell behavior and contributes to tumor progression by promoting an invasive phenotype of cancer cells. Moreover, previous studies have shown that the increased stromal stiffness directly influences the proliferation, migration, and VEGF release of invasive cancer cell lines [30]. In chapter 4, it was shown that increase in mechanical strength of the microenvironment upregulated the release of pro-angiogenic signals by the highly aggressive, highly invasive breast cancer cell line, MDA-MB-231. Previous studies showed that cancer cells with non-aggressive/non-invasive phenotype do not exhibit stiffness-dependent changes in cellular processes [30].

To determine whether the angiogenic release by less aggressive breast cancer cells is dependent on stiffness, MCF-7 cells were encapsulated in soft and stiff collagen gels for 6 days, and their behavior was studied. Their proliferation was tested via DNA quantification over time, and their morphology was examined by confocal imaging. Furthermore, the angiogenesis related molecules released into the culture medium were profiled using the human angiogenesis antibody assay, and the expression of pro- and anti-angiogenic molecules was compared as a function of matrix stiffness.

Results

To study the impact of matrix stiffening on cells of non-aggressive phenotype, MCF-7 cells were incorporated into collagen gels of varying stiffness. DNA quantification was used to assess

the viability of the cells 2, 4, and 6 days post-fabrication. As shown in Figure 9, cell viability did not change despite the change in matrix stiffness. Further, staining F-actin filaments did not reveal any difference in the cytoskeletal organization as a function of matrix stiffness (Fig 10).

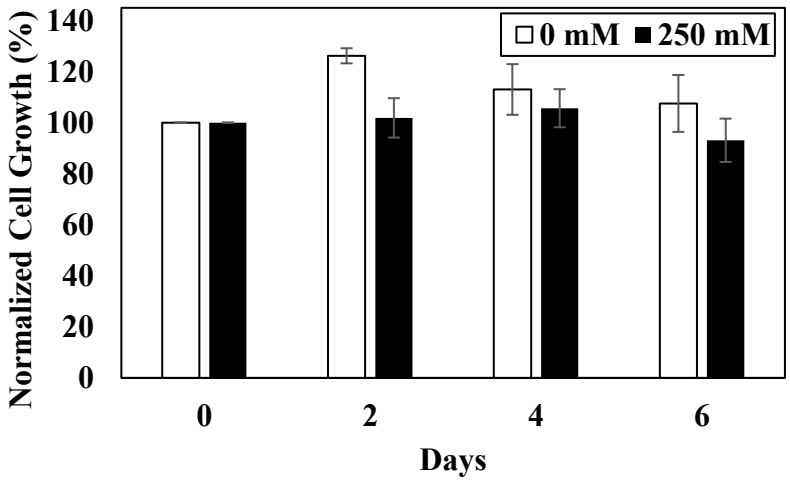

Figure 9. Proliferation of MCF-7 cells encapsulated in glycated (250 mM) and non-glycated (0 mM) gels. Cell growth was assessed after 2, 4, and 6 days and compared to the day of fabrication. Error bar S.E.M (N=3).

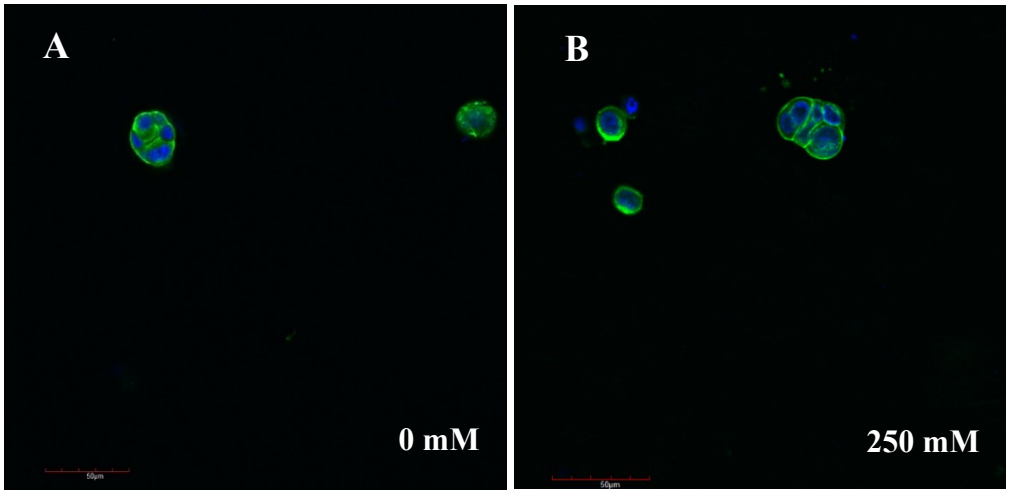

Figure 10. The confocal images of MCF-7 cells in (A) soft and (B) stiff collagen gels displaying the arrangement of actin fibers (green). Hoechst 33342 (blue) stained the nuclei of the cells. The scale bar corresponds to 50 µm.

To investigate the influence of matrix stiffening on the angiogenic activity of MCF-7 cells, 4 days post-fabrication, the conditioned media was collected, and the released angiogenic factors were profiled. The release of pro-angiogenic molecules by MCF-7 cells encapsulated within

collagen gels treated with 250 mM ribose (730 Pa) was compared with those encapsulated with collagen gels without treatment with ribose (0 mM, 175 Pa) (Fig 11A). As observed, the expression of most pro-angiogenesis related factors was unchanged between the stiffer, ribose treated (250 mM, 730 Pa) and soft, untreated (0 mM, 175 Pa) gels with the exception of a few factors (EGF and FGF-7) that were only expressed in the compliant gel and VEGF-C which was only expressed in the stiffer gel. Similarly, the expression of most of the anti-angiogenic factors from the cells in both stiff and compliant gels was unchanged with the exception of endostatin/collagen XVIII which was only expressed in the compliant gel and platelet factor 4 and vasoinhibin which were expressed only in the stiffer gel (Fig 11B).

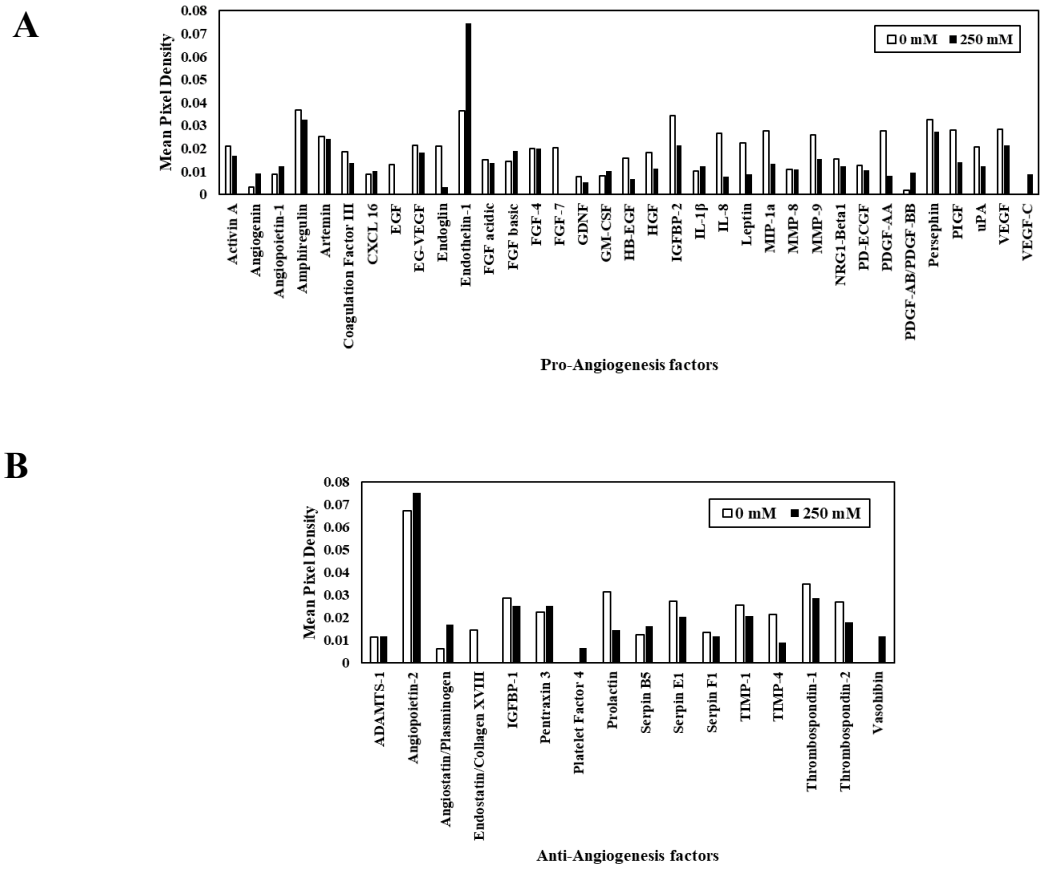

Figure 11. Effect of matrix stiffness on angiogenic activity of MCF-7 cells. The mean pixel density of (A) pro-angiogenic factors and (B) anti-angiogenic factors released by MCF-7 cells encapsulated in compliant (0 mM) and stiff (250 mM) collagen gels assayed via Angiogenesis Proteome Profiler.

Figure 12A and 12B demonstrate the relative expression of the released factors from the stiffer gel compared to the compliant gel. No difference in the expression pattern of most of the pro- as well as anti-angiogenic molecules was observed (0.5< normalized values <1.5), with the exception of angiogenin, endothelin 1, PDGF-AB/BB and angiostatin/plasminogen that were upregulated (normalized values > 1.5) and endoglin, HB-EGF, IL-8, Leptin, MIP 1a, and PDGF-AA and prolactin and TIMP-4 were downregulated (normalized values < 0.5).

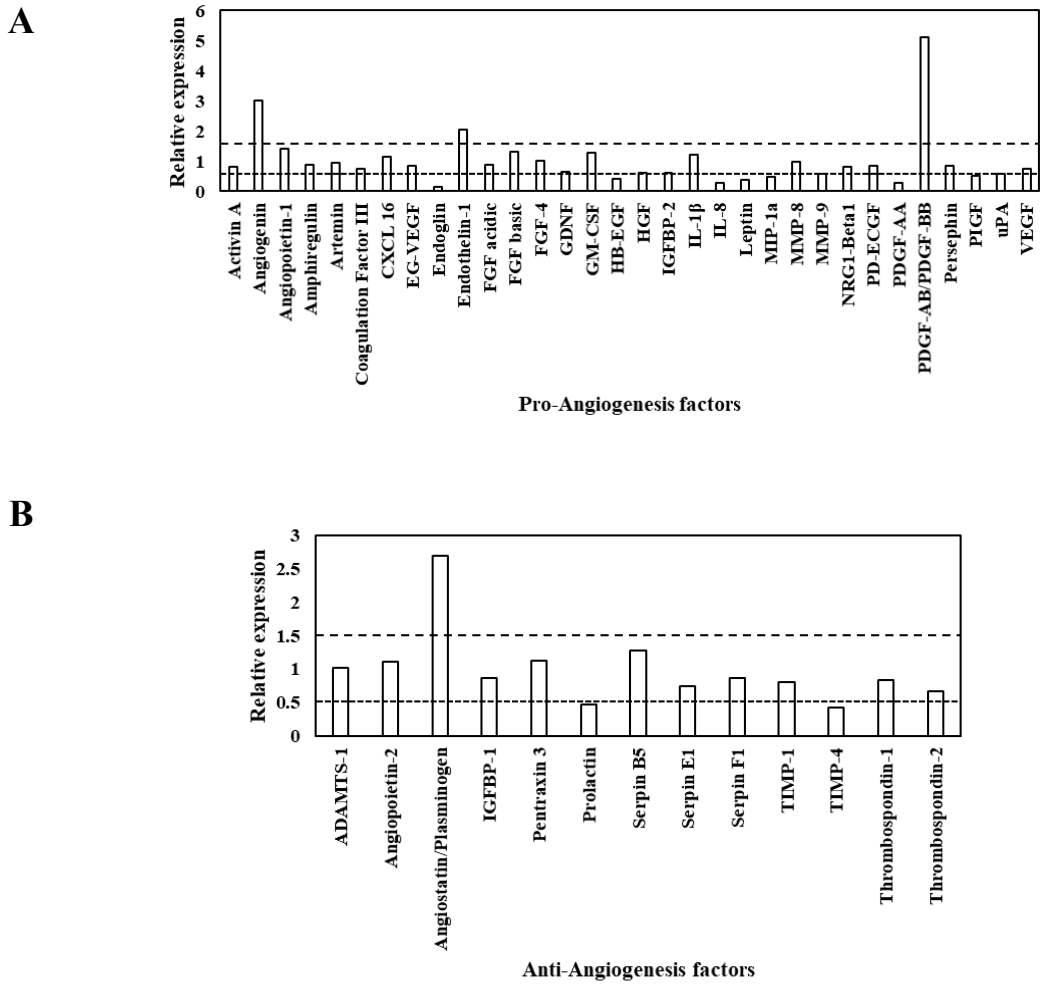

Figure 12. The normalized expression of (A) pro-angiogenic factors and (B) anti-angiogenic factors when MCF-7 where encapsulated in glycated collagen gels relative to non-glycated collagen gels. The closely dashed and widely dashed lines corresponds to the relative expression of 0.5 and 1.5, respectively.

Discussion

In this study, only three pro-angiogenic factors were over expressed by MCF-7 cells encapsulated in the stiffer matrix (angiogenin, endothelin-1, and PDGF-AB/BB), whereas, multiple pro-angiogenic factors were upregulated by invasive cancer cells (activin A, amphiregulin, artemin, IL-1β, persephin, uPA, and VEGF) (in Chapter 4). Amphiregulin, which is an EGF-related peptide, was overexpressed by highly aggressive MDA-MB-231 cancer cells encapsulated in stiffer matrices, but not by the non-aggressive MCF-7 cells encapsulated in stiffer matrices. This is consistent with other studies where the frequency and levels of amphiregulin expression are generally higher in invasive breast tumors than in localized carcinoma or in normal breast tissue [51]. Moreover, MDA-MB-231 exhibited no change in the expression of anti-angiogenic signals with increasing stiffness. On the other hand, MCF-7 encapsulated in stiffer matrices grossly over-expressed angiostatin, a specific angiogenesis inhibitor produced by tumors that blocks tumor angiogenesis and inhibits metastatic and primary tumor growth [52]. While VEGF-C was only expressed by the cells in the stiffer matrices, this is consistent with other studies where VEGF-C in MCF-7 tumors strongly encourages the growth of tumor-associated lymphatic vessels but unlike VEGF, does not have any significant effects on tumor angiogenesis [53]. In comparison to the highly invasive cell line, non-invasive MCF-7 cells did not exhibit a significant alteration in the angiogenic signaling as a function of matrix stiffness. These results are in agreement with the trend observed in earlier 2D studies whereby substrate stiffness-dependent VEGF expression by MDA-MB-231 cells was observed [30].

Chapter 6: Effect of Mechanotransduction Inhibitors on Angiogenic Activity

Introduction

In Chapter 4, we observed formation of actin-based protrusion of plasma membranes when MDA-MB-231 cells were encapsulated within the stiffer gels. On the other hand, no difference in morphology or cytoskeletal arrangement was observed in case of MCF-7 cells. This observation along with the angiogenesis results discussed in Chapter 4 suggests that differential secretory responses of MDA-MB-231 cells may be partly related to the cell contractility or cytoskeletal reorganization. Previous studies demonstrated that the change in mechanical properties of the microenvironment increase integrin clustering and recruitment of focal adhesion proteins leading to cytoskeletal reorganization [24, 54, 55]. These changes result in activation of the Rho/ROCK pathways. In an earlier study, Rho associated kinase (ROCK) inhibition decreased substrate stiffness-dependent increase in proliferation and migration of cells as well as significantly reduced the release of VEGF [30]. This suggests that the signaling pathways and their effect on cytoskeletal reorganization may have an important function in tumor angiogenesis.

To study the effect of inhibiting mechanotransduction pathways on the pro-angiogenesis release of cancer cells with invasive phenotype, three inhibitors, each affecting the mechanical signaling pathway were added to the cells. Since it was shown earlier that aggressive cancer cells in stiff matrices exhibited an increase in pro-angiogenesis signaling, the inhibitors were added to MDA-MB-231 cells in stiff matrices, only. Specifically, Y-27632, Blebbistatin, and Cytochalasin D inhibitors were used. Y-27632 is a widely used Rho/ROCK inhibitor that binds to the catalytic site of these kinases thereby inhibiting their activity and the formation of stress fibers [56].

Blebbistatin is a myosin II inhibitor that binds to the myosin-ADP-P_i complex and interferes with the phosphate release process, thereby preventing proper crosslinking of actomyosin [57]. Cytochalasin D is a widely used actin inhibitor that inhibits both the polymerization and depolymerization of actin subunits by binding to actin filament ends [58]. The angiogenesis release profile from cells incubated with the different inhibitors was assessed, and the effect of the inhibitors on cell viability was also determined.

Methods

Inhibition of Mechanotransduction Pathways

Cancer cells were embedded into collagen gels at a density of 12.5 x 10^4 cells/gel and incubated in serum-free media for 48 hours at 37°C and 5% CO_2. Following which, serum-free media containing either 10μM of Y-27632, 50 μM of Blebbistatin, or 1μM of Cytochalasin D, inhibitors targeting the mechanotransduction pathway, were added to the cells embedded into stiff collagen matrices. The cells were incubated with the different inhibitors for 48 hours at 37°C and 5% CO_2. Cells incubated in serum-free media without any inhibitors served as the control. The cell viability was assessed using AlamarBlue™ Cell Viability Reagent for 3.5 hours, and the fluorescence intensity was measured at excitation/emission wavelengths 570/595 nm to ensure that the inhibitors were not toxic to the cells. Following incubation for 48 hours, the media was collected, concentrated, and the profile of the released angiogenic factors was assessed via Proteome Profiler™ Human Angiogenesis Array from R&D Systems as described earlier.

Results

After 48 hours of incubation with the inhibitors, the serum-free media was collected and assessed for the released angiogenic factors. Figure 13 shows the normalized signal intensities of the factors released by cells from gels in presence of inhibitors with respect to those released in the absence of inhibitors. Y-27632, downregulated the expression of multiple molecules including

angiogenin, angiopoietin-1, amphiregulin, artemin, FGF acidic, GDNF, GM-CSF, IGFBP-1, IL-1β, MIP-1a, MMP-8, PD-ECGF, PDGF-AA, PDGF-AB/BB, uPA, VEGF (pro-angiogenic factors) (Fig 13). On the other hand, in the presence of Blebbistatin and Cytochalasin D, the expression of multiple pro-angiogenic molecules were upregulated.

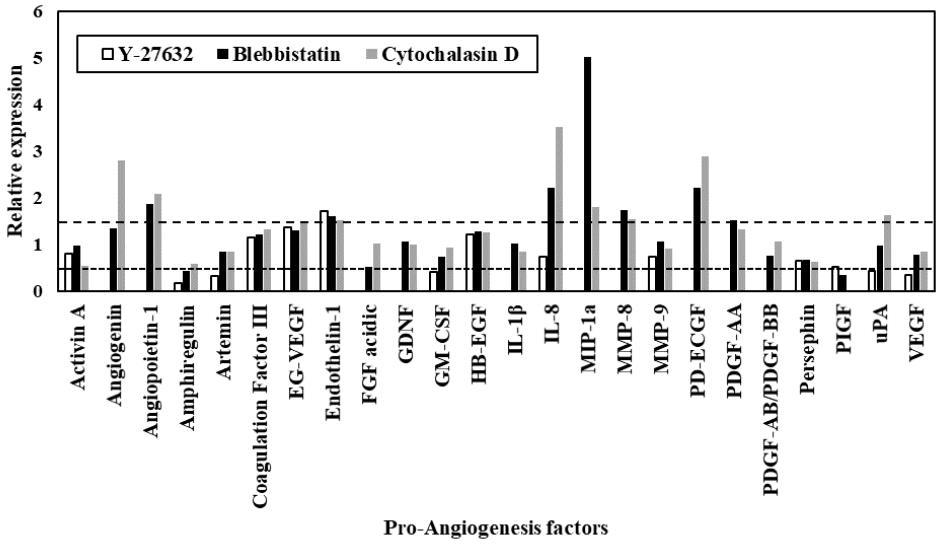

Figure 13. Effect of mechanotransduction inhibitors on pro-angiogenic signaling of MDA-MB-231 encapsulated in stiff (250 mM) collagen gels. The normalized expression of pro-angiogenic factors when MDA-MB-231 cells were incubated with 10μM of Y-27632, 50 μM of Blebbistatin, or 1μM of Cytochalasin D relative to cells incubated without inhibitors. The closely dashed and widely dashed lines corresponds to the relative expression of 0.5 and 1.5, respectively.

The cell viability was tested to assess whether the alteration in angiogenic signaling is due to the cytotoxicity of the pharmacological inhibitors. However, no difference in the viability of the cells incubated in the presence of different inhibitors was observed when compared to those incubated in the absence of inhibitors (Fig 14). This suggests that differential expression of angiogenesis-related factors by MDA-MB-231 in the presence of pharmacological inhibitors can be attributed only to the inhibition of mechanotransduction events.

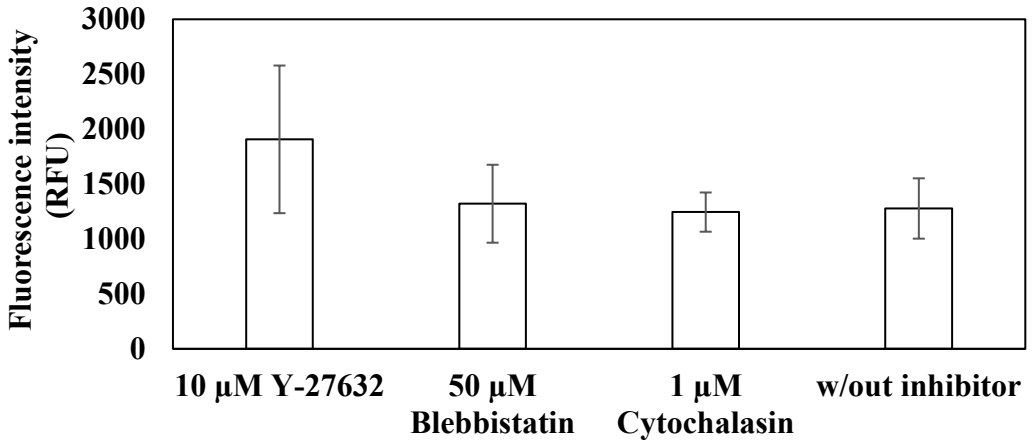

Figure 14. The cell viability of MDA-MB-231 cells in stiff (250 mM) matrices incubated with and without inhibitors. Inhibitors did not affect cell viability. Error bar S.E.M (N=3).

Discussion

The local interactions between F-actin, myosin filaments, and various crosslinking proteins govern force generation, dynamics, and reorganization of the intracellular cytoskeleton. The cytoskeleton is responsible for many essential cellular functions including migration, adhesion, and mechanotransduction (59). Our study demonstrated that ROCK inhibitor, Y-27632, downregulated the expression of the pro-angiogenic factors, suggesting the involvement of ROCK signaling pathway in the stiffness-dependent pro-angiogenic signaling of MDA-MB-231 cells. On the contrary, Blebbistatin and Cytochalasin D upregulated the expression of different pro-angiogenic molecules. Although this was somewhat unexpected, we anticipate that different mechanisms by which actin filament disruptors and myosin inhibitor affect the cytoskeleton may play a role in the angiogenic activity of the cancer cells. Y-27632 is a specific inhibitor of ROCK activity. As a major effector of RhoA, ROCK modulates actin cytoskeleton organization, stress fiber formation, and smooth muscle contraction via phosphorylation of myosin light chain (MLC) and LIM kinase (LIMK) and has been associated with matrix-stiffness induced mechanotransduction (56). Previous study using ROCK inhibitor reported that ROCK activity is

essential for stress fiber formation and various cellular functions (30). Blebbistatin selectively inhibits non-muscle myosin II in an actin-detached state (57) thereby inhibiting ATP-binding required for motor activity and actin cross-linking, independently of MLC phosphorylation (60). On the other hand, Cytochalasin D inhibits actin polymerization and induces depolymerization of actin filaments (59). The data above shows that neither the inhibition of non-muscle myosin II nor the inhibition of actin polymerization govern the pro-angiogenic signaling of MDA-MB-231 cells. Instead, this study shows that the angiogenic activity of the breast cancer cells is dependent on the activation of Rho/ROCK pathway.

Chapter 7: Conclusion

In this study, collagen hydrogels of varying stiffness were fabricated using a non-enzymatic glycation approach and characterized. Highly invasive breast cancer cells, MDA-MB-231, were encapsulated in soft (non-glycated) and stiff (glycated) matrices. Stiffer microenvironments resulted in an increase of pro-angiogenic signaling and the expression of many angiogenesis-related factors not expressed in soft matrices. The change in stiffness, however, did not alter the anti-angiogenic signaling by the aggressive cancer cells. Furthermore, the bioactivity of the released angiogenesis factors was assessed through the proliferation of HUVECs cells. The observed increase in their proliferation in presence of conditioned media from stiffer gels was not statistically significant. We also investigated whether the stiffness-dependent secretory activity of breast cancer cells can be correlated to their aggressive phenotype. Towards this, breast cancer cells of low invasiveness were encapsulated in soft and stiff collagen gels, and their angiogenic signaling was minimally altered. This reveals differential responses of breast cancer cells displaying varying degrees of invasiveness to changes in stromal stiffening. Furthermore, the increase in pro-angiogenic activity in cancer cells subject to increased substrate stiffness indicates the existence of a mechanotransduction pathway that has not only been shown to regulate cell behavior but also suggests its potential regulatory role in angiogenesis. Highly aggressive breast cancer cells in stiff matrices were incubated with three different inhibitors. Y-27632, ROCK inhibitor, significantly interrupted the pro-angiogenic release, while Blebbistatin, myosin II inhibitor, and Cytochalasin D, actin polymerization inhibitor, did not inhibit the release of pro-angiogenic factors by the cancer cells. This suggests that the angiogenic activity of breast

cancer cells is dependent on the activation of Rho/ROCK pathway, and interfering with this pathway may play a therapeutic role in disrupting tumor angiogenesis.

SECTION II

ROLE OF MICROENVIRONMENT IN CANCER METASTASIS

Chapter 8: Motivation and Objectives

At initial diagnosis with breast cancer, up to 5% of patients present with distal metastases, and an additional 10-15% develop metastases within three years of diagnosis [61]. Metastasis is the spread of cancer cells from the primary tumor location to surrounding and distant tissues and is responsible for 90% of cancer deaths. Bone metastasis is characterized by severe pain, impaired mobility, fractures, spinal cord compression, bone marrow aplasia and hypercalcemia and results in an average survival period of 19-25 months upon metastasis from breast cancer [63]. Once metastasis occurs, it becomes hard to control and cure the disease, and treatment becomes more focused on slowing disease progression and alleviating pain. Therefore, it is important to acquire a better understanding of bone metastasis in order to develop effective treatments for metastasized tumors.

In order for the cancer cells to thrive in the foreign microenvironment and progress to form lesions and proliferate, the extravasated tumor cells need to manipulate and recruit the resident host cells in the bone marrow, namely osteoblasts and osteoclasts. They do so by secreting osteolytic factors that directly stimulate bone resorption by osteoclasts and indirectly promoting osteoclastogenesis via upregulation of RANKL signaling by osteoblasts [11]. This results in the increased osteolysis that is characteristic of bone metastasis from primary breast tissue. Tumors also affect stromal cells in the bone marrow that can differentiate into osteoblasts, osteoclasts, or adipose cells [11]. Furthermore, as mentioned earlier, tumor cells also secrete angiogenic factors that allow blood vessel formation to occur to support the ever-growing demand of more nutrients and oxygen by the proliferating and growing tumor.

The ability to identify molecular factors that influence the establishment and progression of tumor cells in bone tissue is of key importance in the development of novel methods for the treatment of bone metastasis. Although animal models provide an *in vivo* model for metastasis research and the understanding of microenvironment-mediated pathways, they also pose a series of complexities, such as uncontrolled variables, lack of human physiology, and variability across different models [63]. *In vitro* models, on the other hand, can either be oversimplified or highly complex, yet expensive and require specially equipped laboratories.

Two-dimensional (2D) systems, although cost efficient and simple, fail to capture the dynamic interactions between the cells and their microenvironment which undergoes constant remodeling by the cells and affects cell behavior. As a result, testing done on 2D models cannot be indicative of results in a more complex *in vivo* system, such as the human body [63]. In recent years, several attempts have been made to develop three-dimensional (3D) models for studying bone metastasis. These models often combine host cells, mesenchymal stem cells or osteoblasts, with tumor cells in artificial scaffolds. While these models demonstrate a significant improvement over 2D systems, they lack natural bone microenvironment or well-controlled spatial distribution of cancer cells [63]. As a result, these 3D systems limit our ability to effectively study early stages of metastasis and bone microenvironment interactions with the invading tumor cells. Because bone metastasis is still incurable and poorly understood, there is a pressing need for a cost-efficient, yet innovative, *in vitro* model complex enough to simulate the tumor environment and mechanical characteristics of *in vivo* biology for the development and screening of new therapeutic drugs.

We hypothesize that utilization of decellularized ECM (dECM), that preserves the natural composition and structure, will permit bioprinting physiologically relevant 3D model of breast cancer metastasis to bone. Thus, this study is aimed at generating structurally preserved bone-like

microenvironments that permit the understanding of cancer behavior during the early stages of metastasis. The research conducted in this work addressed the following two objectives:

Objective 1: Characterize dECM obtained from osteogenesis-differentiated mesenchymal stem cells (MSCs)

Bone marrow-derived human MSCs were osteogenically differentiated for 21 days. The generated matrices were decellularized and characterized to determine their composition.

Objective 2: Test effect dECM and tumor interaction on the behavior of highly aggressive cancer cells.

MDA-MB-231 cells were seeded on osteogenic differentiated and undifferentiated dECM. Their cell proliferation was assessed. Additionally, the inhibitory effect of chemotherapy drug, 5-fluorouracil, on the cancer cells was examined.

Chapter 9: Characterization of dECM

Introduction

The bone microenvironment consists of a variety of cells including endothelial, immune, and hematopoietic and bone marrow stem cells [64]. However, the extracellular matrix (ECM), produced by osteoblasts, makes up the bulk of the bone's dry weight. Osteoblasts are bone cells, derived from the differentiation of mesenchymal stem cells (MSCs), that play a role in bone remodeling, bone mineralization, as well as the production of ECM components [65, 66, 67]. Bone matrix consists of organic and mineralized inorganic components. The mineralized inorganic part of the ECM consists of calcium and phosphate in the form of hydroxyapatite crystals that provide the bone tissue with specific properties, such as rigidity and hardness [64]. Meanwhile, the organic component of the ECM encompasses three major biomolecules: fibrous proteins, glycoproteins, and proteoglycans.

Collagen fibers account for nearly 90% of the proteins in bone ECM, with collagen type I as the most common form. In addition to its role in biochemical signaling, the collagen matrix provides the bone with strength and stability as well as a scaffold for cells to attach and form bone tissue [65, 66, 68]. Collagen fibers are composed of densely packed molecules with a triple helical structure that arrange in a directional manner reflecting the cell's orientation [65, 69, 70, 71]. The properties provided by the organization of these fibers dictate many cellular behaviors, such as proliferation, migration, and differentiation [65, 72, 73].

Glycoproteins within the matrix, specifically fibronectin, facilitate cell-matrix interaction, namely cell adhesion, migration, and differentiation [65, 74]. In the bone, fibronectin is produced

by osteoblasts and has been shown to induce the osteogenic differentiation of MSCs [65, 76]. Additionally, fibronectin mediates the formation of collagen fibers through its collagen binding domain [65, 74].

Proteoglycans are a major component of the ECM and are essential for regulated bone matrix formation. They modulate cell signaling through the binding of proteins to either enhance, diminish, or inhibit their signal, or by preventing the degradation of proteins [2, 69]. Proteoglycans consist of side sugar chains, glycosaminoglycans (GAGs), that are bound to a core protein. GAGs play an important role in the bone matrix by regulating the availability and activity of many osteoclastic and osteogenic factors [77].

To study bone metastasis of breast cancer using naturally derived bone microenvironments, bone-marrow derived MSCs were differentiated into osteoblasts. Successful osteogenic differentiation was confirmed by detection of alkaline phosphatase activity and extracellular calcium deposits via Alizarin Red S staining. Further, the deposited ECM by osteoblasts was decellularized and characterized to determine if successful deposition of key bone matrix components occurred. Specifically, the decellularized ECM (dECM) was examined to verify the deposition of collagen, fibronectin, and sulfated glycosaminoglycans.

Methods

Osteogenic Differentiation of MSCs

Mesenchymal stem cells (MSCs), derived from bone marrow, were purchased from American Type Culture Collection (ATCC) and cultured in Dulbecco's Modified Eagle Medium (DMEM, Gibco, NY) supplemented with 10% (v/v) fetal bovine serum (FBS) and 1% (v/v) penicillin-streptomycin at 37℃ and 5% CO_2. Cells were detached from flasks using 0.25% Trypsin-EDTA, and resuspended MSCs were seeded in 6 well plates at a density of 5 x 10^4

cells/well. The cells were cultured in complete DMEM media for 72 hours, or until they reached confluency. Following which, differentiation media consisting of Stem Pro Osteocyte/Chondrocyte Differentiation Basal Medium (Gibco, NY), 10% (v/v) StemPro Osteogenesis Supplement (Gibco, NY), and 1% (v/v) penicillin-streptomycin was added to the cells and replaced every 3 days for a total differentiation period of 21 days. MSCs cultured for 21 days in complete DMEM media served as the control.

Confirmation of Osteogenic Differentiation

Osteogenic differentiation was confirmed using Alkaline Phosphatase test and Alizarin Red S Staining. Alkaline phosphatase test was carried out after 9 days of differentiation. Briefly, the cells were fixed with 1:1 acetone:methanol at -20℃ for a maximum of 90 seconds to avoid inactivation of alkaline phosphatase. The fixed cells were then rinsed with washing buffer consisting of 0.05% Tween 20 in DPBS for 45 seconds and incubated with alkaline dye mixture at room temperature for 30 minutes in the dark. To prepare the alkaline dye mixture, Fast Blue RR Salt pre-weighed capsule (Sigma Aldrich, MO) was dissolved in 48 mL of distilled water to prepare diazonium salt solution. 2 mL of Naphthol As-MX Phosphate Alkaline solution was added to the diluted diazonium salt solution. After incubation, the cells were washed with distilled water for 3 minutes, and DPBS was added to the wells. The cells were imaged using Zeiss Axio Observer A1 microscope with integrated CCD camera.

Alizarin Red S Staining was carried out after 21 days of differentiation. The cells were fixed with 1:1 acetone:methanol solution at -20℃ for 20 min and washed with DPBS. 2% (v/v) Alizarin Red S staining solution was added to the fixed cells and incubated at room temperature for 45 min in the dark. The staining solution was prepared by dissolving Alizarin Red S in distilled water, and the pH was adjusted with 1 M HCl to achieve a pH range of 4.1-4.3. After 45 minutes,

the cells were washed four times with distilled water and replenished with DPBS for imaging.

Deposition and Decellularization of dECM

MSCs were seeded in Lab-Tek chamber slides at a density of 1.5 x 10^4 cells/chamber and cultured until confluency with complete DMEM medium. After confluency, the cells were cultured in osteogenesis differentiation media or normal DMEM media. After 21 days, the cells were treated with 0.5% Triton-X-100 (Sigma-Aldrich, MO) in 20 mM ammonium hydroxide (NH_4OH, Fisher Scientific, NJ) for 10 minutes at 37°C, as described earlier [78]. The wells were then washed with DPBS for 5 minutes and treated with 200µg/mL DNase I, RNase-Free (OPTIZYME, FisherBioReagents), for 60 minutes at 37°C. Following which, the wells were rinsed with DPBS for 5 minutes and left to air dry overnight to allow for good visualization of dECM. Phase contrast images of the dried ECM were then captured.

Immunostaining

Immunofluorescence staining was carried out as described previously [78]. The decellularized ECM (dECM) was fixed using a 1:1 methanol:acetone solution at -20°C for 20 minutes and washed once with DPBS. The fixed dECM was blocked with 5% BSA for 1 h at room temperature on an orbital shaker and washed once with DPBS. The samples were then incubated overnight with COL1A1 antibody (Santa Cruz biotechnology) and monoclonal anti-fibronectin antibody (Sigma Aldrich, MO). The samples were rinsed once with DPBS and incubated with secondary antibody for 1h at room temperature. Following which the samples were washed, and confocal images of collagen and fibronectin in the dECM were captured.

Quantification of Deposited Collagen in dECM

To determine the concentration of deposited collagen in dECM, a Soluble Collagen Assay Kit (Cell BioLabs, CA) was utilized. Briefly, dECM samples in 6 well plates were incubated with

0.5mg/mL of pepsin (Sigma-Aldrich, MO) solution in 0.5M acetic acid overnight at 4℃. 100µL duplicates of digested dECM samples and collagen standards were transferred to the wells of a 96 well plate and allowed to dry at 37℃ overnight. Sirius Red reagent was added to the wells at room temperature for 1 h on an orbital shaker to stain the collagen, and the stained samples were washed with 5% acetic acid and incubated with an extraction solution for 30 minutes. The collagen concentration was determined by measuring the absorbance using SpectraMax M3 Multi-Mode Microplate Reader at a wavelength of 550 nm.

Quantification of Sulfated Glycosaminoglycans

The amount of deposited sulfated glycosaminoglycans (GAGs) in the dECM was determined using Glycosaminoglycans Assay Kit (Chondrex, Inc., WA). First, dECM samples were digested with papain extraction reagent for 3 h at 37℃ to extract the sulfated GAGs. 100 µL duplicates of digested dECM, along with standards, was added to 96 well plates. 1,9 Dimethylmethylene Blue (DMB) dye solution was added to the samples, and the absorbance was measured using BioTek Eon Microplate reader at a wavelength of 525 nm to determine the concentration of GAGs in the samples.

Results and Discussion

Before isolating the ECM from the osteogenic differentiated cells, it was important to first determine that the differentiation process used was successful. Undifferentiated mesenchymal stem cells (MSCs) display weak alkaline phosphatase (AP) activity, whereas differentiated osteoblasts show very high AP activity. As shown in Figure 15A, insoluble precipitates formed after 9 days of differentiation, confirming alkaline phosphatase activity at those sites, but were not visible in undifferentiated MSCs (Fig 15B). Moreover, differentiated osteoblasts exhibit extensive extracellular calcium deposits during bone formation, while undifferentiated MSCs do not deposit

calcium. Using Alizarin Red S, calcium deposits stain bright orange-red as shown in the image of differentiated MSCs in Figure 15C, whereas undifferentiated cells were colorless (Fig 15D). Together, alkaline phosphatase activity and calcium deposits indicate the successful differentiation of MSCs into osteoblasts.

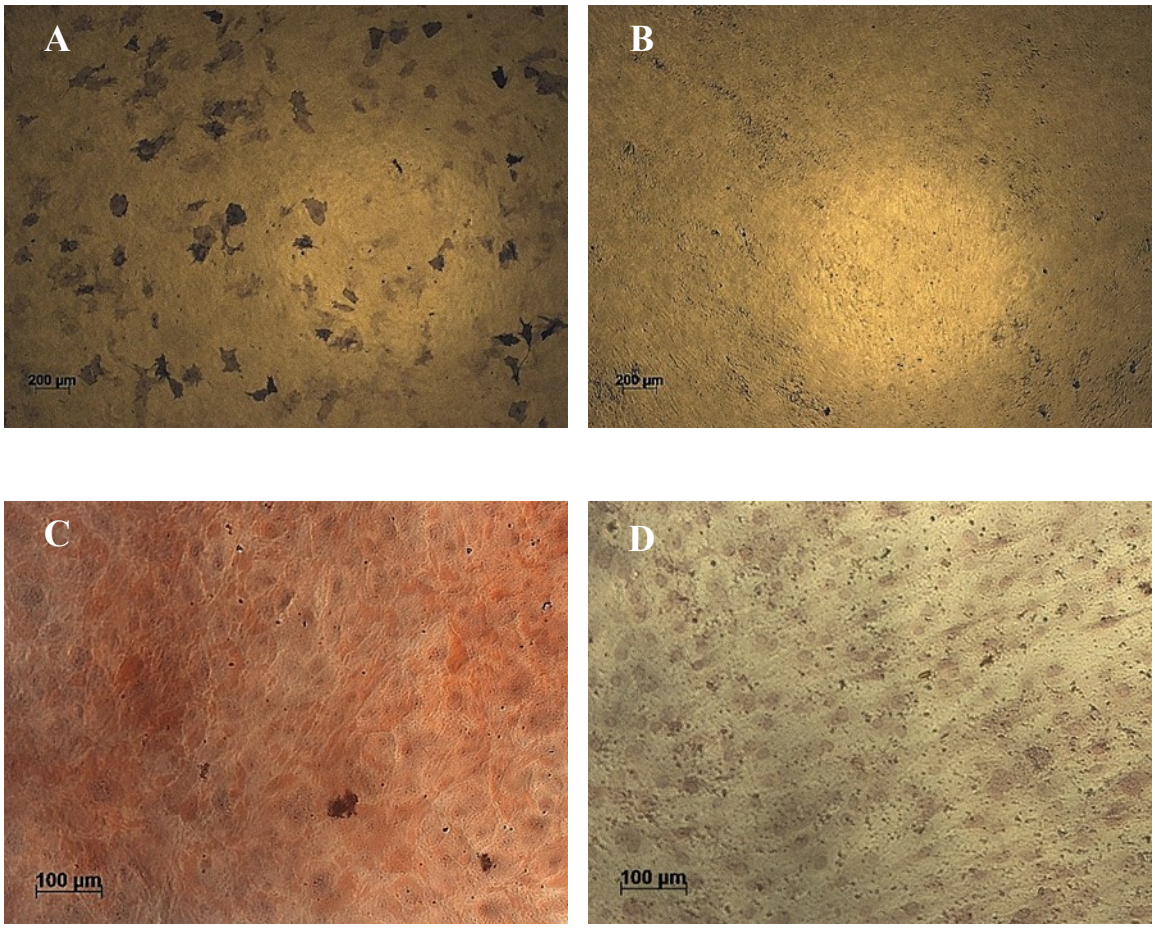

Figure 15. Confirmation of osteognic differentiation of MSCs. Alkaline phophatase test detected insolube precipitates indicating AP activity in (A) differentiated MSCs, but did not detect any enzyme activity in (B) undifferentiated MSCs. Scale bar corresponds to 200µm. Alizarin Red S staining was performed to check for calcium deposits. (C) Differentiated MSCs stained a bright red indicating the presence of calcium deposits, while (D) undifferentiated MSCs remained colorless, indicating no extracellular calcium depostition. Scale bar corresponds to 100µm.

The methods utilized in this study led to cellular deposition of ECM, which was structurally preserved during the decellularization process. Figure 16 shows phase contrast images of the dried ECM network that remained in the wells after treatment with detergent. The ECM secreted by

MSC-derived osteoblasts show a more visibly dense network (Fig 16A) than what was deposited by undifferentiated MSCs (Fig 16B).

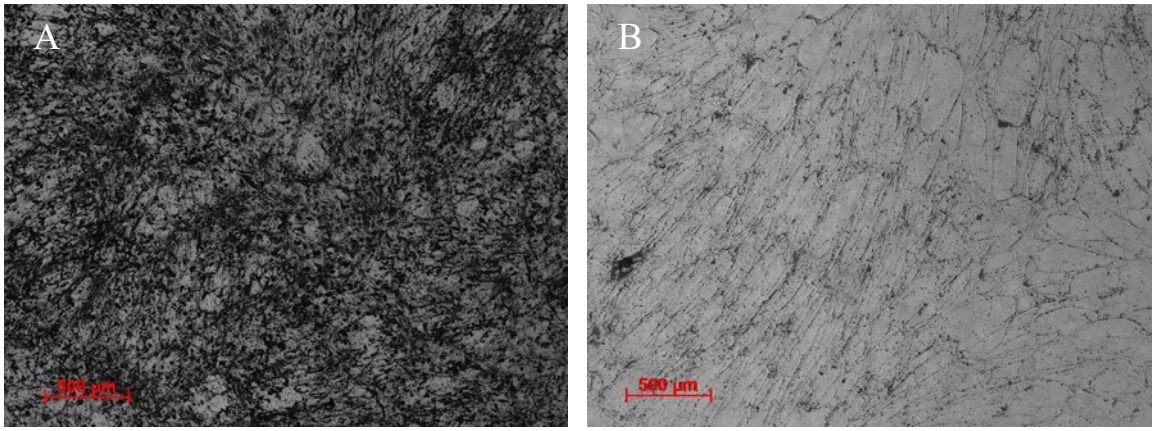

Figure 16. Phase contrast images of deposited ECM after decellularization of (A) differentiated MSCs and (B) undifferentiated MSCs. Scale bar corresponds to 500µm.

Since the differentiated MSCs appeared to deposit a denser ECM network than the layer deposited by undifferentiated MSCs, the decellularized matrix was characterized to determine the difference in the amount of secreted ECM components. For this purpose, the dECM was stained for collagen and fibronectin, two of the major structural proteins of the extracellular matrix. Confocal images in Figure 17 of stained dECM showed that collagen and fibronectin were deposited more heavily by osteogenic differentiated MSCs than undifferentiated cells.

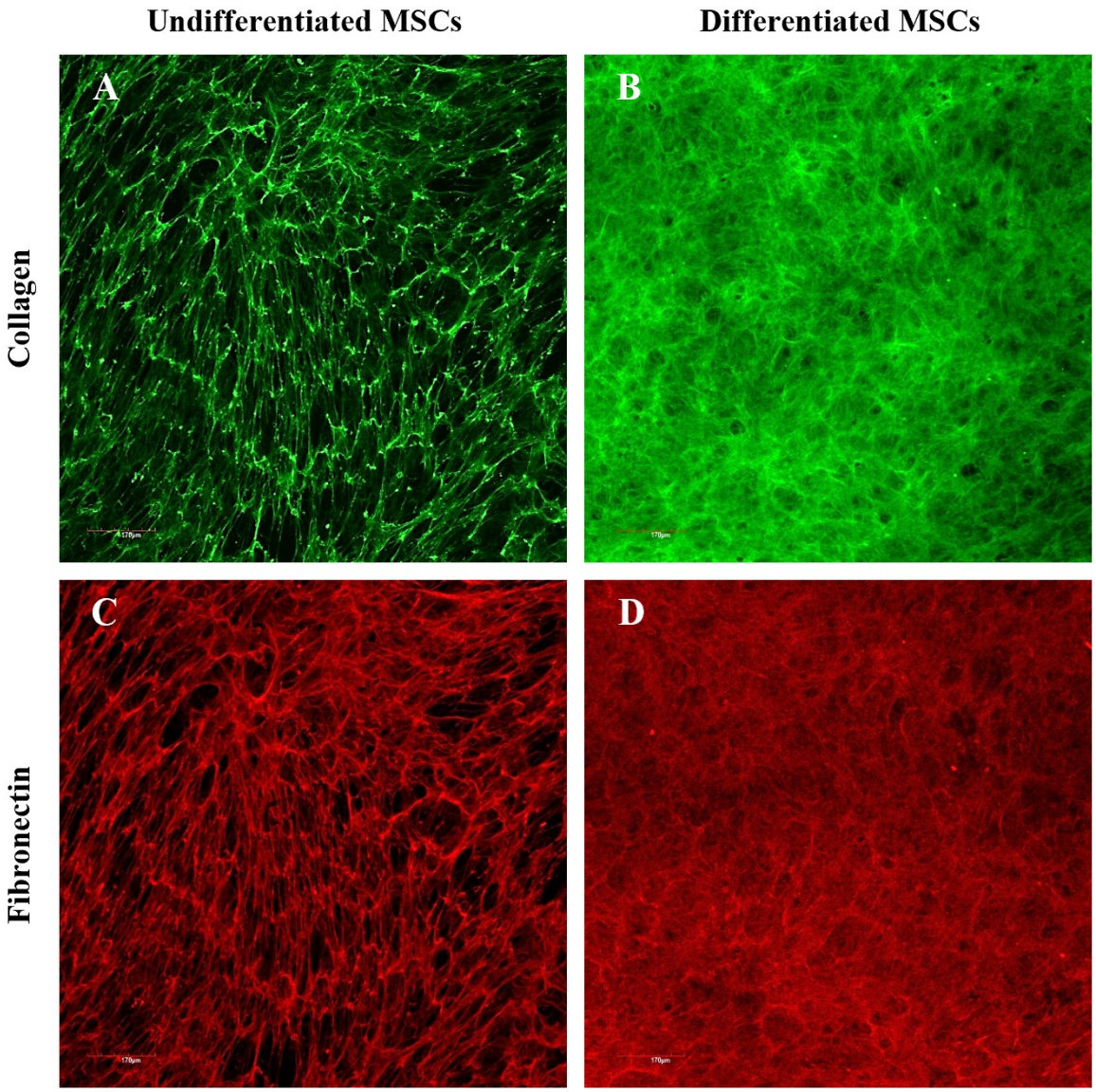

Figure 17. Confocal images of immunofluorescence stain of collagen and fibronectin in decellularized ECM of undifferentiated and differentiated MSCs. Immunostaining of collagen showed less deposition by (A) undifferentiated MSCs compared to (B) differentiated osteoblasts. Immunostaining of fibronectin in dECM also showed less deposition by (C) undifferentiated MSCs compared to (D) differentiated osteoblasts. Scale bar corresponds to 170 µm.

To further demonstrate the visible disparity in protein deposition in the dECM of osteogenic differentiated and undifferentiated MSCs, the concentration of collagen was quantitatively determined. The decellularized matrix of differentiated osteoblasts contained a greater concentration of collagen in comparison to the undifferentiated MSCs (Fig 18A). Moreover, the concentration of deposited proteoglycans was assayed. Osteoblasts secreted more

sulfated glycosaminoglycans into the ECM than MSCs (Fig 18B). The increase in, both, collagen and sulfated GAGs was statistically insignificant (p-value > 0.05).

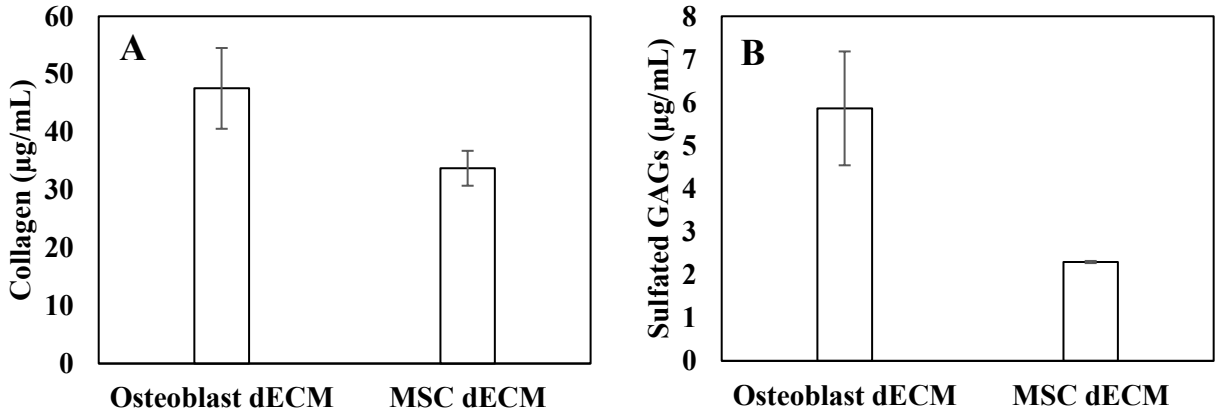

Figure 18. Quantification of the concentration of deposited (A) collagen and (B) sulfated glycosaminoglycans in the decellularized matrices of differentiated osteoblasts and undifferentiated MSCs. Error bar S.E.M (N=3).

The results shown above indicate that the methods used in this section allow the production of bone-like environments containing critical components of the extracellular matrix, such as collagen, fibronectin, and GAGs. More importantly, this provides a model that can replicate the *in vivo* bone environment that breast cancer cells invade during the initial stages of lesion formation. Bone metastatic cancer has been shown to change the production and orientation of collagen, thereby disrupting proper bone structure and function. Specifically, tumor cells result in an increased deposition of dense, misaligned collagen fibers at the site of invasion resulting in bone weakness [65]. Furthermore, fibronectin production is also altered by cancer cells, which release signals that drive native cells to produce a highly unorganized matrix of thick, dense fibronectin fibrils [65, 79, 80].

Chapter 10: Effect of dECM on Aggressive Breast Cancer Cells

Introduction

The bone matrix is under constant remodeling, with a balance between degradation of ECM components by osteoclasts or secretion by osteoblasts, to maintain an optimum bone density and strength [64, 65]. However, due to bone metastasis, these normal processes are disrupted. Tumor cells stimulate osteoclasts to resorb part of the ECM [11] and recruit osteoblasts such that they deposit collagen type I and other ECM components in a highly disordered manner leading to a stiff and unorganized matrix [65]. This change in matrix structure promotes tumor growth and invasion.

In this study, the impact of bone matrix on the behavior of highly aggressive breast cancer is investigated. Previous studies showed that the presence of a mineralized matrix enhances cancer cell adhesion and proliferation [81]. Furthermore, recent evidence suggests that the tumor microenvironment plays a role in the cell's resistance to drugs [82]. Here, the effect of osteoblast-derived ECM on the proliferation of MDA-MB-231 cancer cells was studied. Moreover, the efficacy of chemotherapeutic drug, 5-fluorouracil, on the cells was tested.

Methods

Proliferation of Aggressive Breast Cancer Cells on dECM

dECM of osteogenic differentiated and undifferentiated MSCs was generated in 48 well plates as described earlier. MDA-MB-231 breast cancer cells were seeded on dried dECM at a density of 2×10^4 cells/well and incubated in complete RPMI media for 72 hours. Cell seeded on tissue culture plate (TCP) with no dECM served as the control. Cell proliferation was assessed

using AlamarBlue Cell Viability Reagent. The proliferation of cancer cells on dECM was expressed as percent growth over the control.

Determining Change in Efficacy of Chemotherapeutic Agent

MDA-MB-231 cells were again seeded on differentiated and undifferentiated dECM in 48 well plates at a density of 2 x 10^4 cells/well and incubated in complete RPMI medium for 24 hours. Cancer cells seeded on tissue culture plate (TCP) served as the control. After the cells were established on the dECM, 50 mg/mL of 5-fluorouracil (5-FU, Sigma-Aldrich, MO) stock solution in dimethyl sulfoxide (DMSO, Sigma-Aldrich, France) was diluted in RPMI medium to achieve varying concentrations (0µg/mL-50µg/mL) and added to the cells. To prevent any confounding effects, DMSO was maintained at a concentration of 0.1% in the final drug solutions. The cells were replenished with fresh media containing 5-FU 48 h after initially introducing the drug and again at 72 h. The cell viability was measured after 96 hours of incubation with the chemotherapeutic agent.

Results and Discussion

The effect of dECM from differentiated osteoblasts and undifferentiated MSCs on the proliferation of highly invasive breast cancer cells was determined. MDA-MB-231 cancer cells were seeded on dECM and TCP (control), and their growth was measured after 72 hours relative to the control. Although not statistically significant ($p > 0.05$), cancer cells seeded on osteoblast-derived dECM exhibited an increase in proliferation compared to undifferentiated MSC derived dECM (Fig 19). The increase in proliferation of cancer cells seeded on bone dECM compared to no ECM was observed in other studies where cells were seeded on porous poly(lactide-co-glycolide) (PLG) scaffolds containing nanoparticles with hydroxyapatite [83]. Another study found that the mineralization of porous poly vinyl alcohol (PVA) scaffolds resulted in the adhesion and proliferation of MDA-MB-231 cells [4].

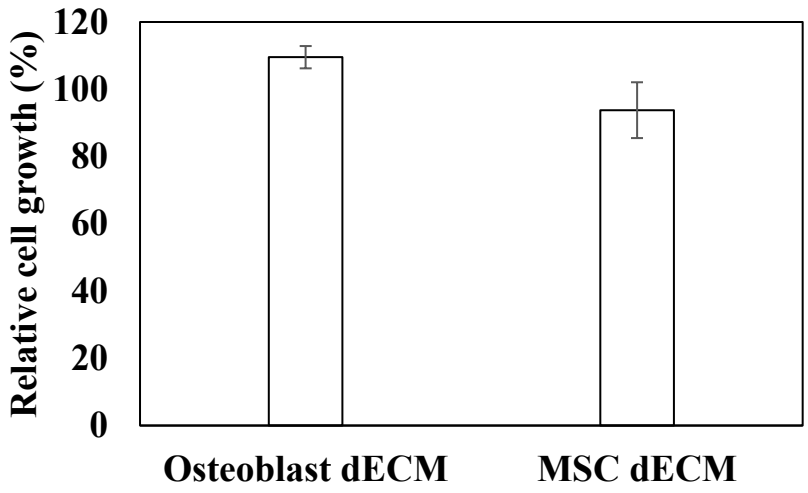

Figure 19. Proliferation of MDA-MB-231 cancer cells on decellularized ECM of differentiated osteoblasts and undifferentiated MSCs. Cell growth was normalized relative to cells seeded on wells with no ECM. Error bar S.E.M (N=3).

Recent evidence suggests that the tumor environment not only regulates the behavior of cancer cells and promotes tumor progression, but it also is involved in the drug resistance properties acquired by cancer cells [82, 84]. Environment-mediated drug resistance is believed to be a result of chemical and mechanical cues as well as the interaction of the tumor with stromal cells and interaction with the extracellular environment [82]. Therefore, to test the efficacy of chemotherapeutic agents in inhibiting tumor colonization of the bone microenvironment, MDA-MB-231 cells were seeded on the decellularized matrices from osteoblasts and MSCs as well as TCP for comparison. The tumor cells were allowed to establish for 24 h in growth medium before being challenged with anti-cancer agents. Following attachment, the cells were treated with chemotherapy drug, 5-fluorouracil (5-FU). The concentration of the drug was varied from 0-50 µg/mL. After 96 hours of incubation with the drug, the cell viability of the cancer cells was measured. Cancer cells seeded on the dECM of both osteoblasts and MSCs exhibited a significant decrease in sensitivity (p-value < 0.05) to the drug in comparison to cells that were seeded on TCP as can be seen from Figure 20. This is consistent with other studies which showed that an increase

in the concentration of chemotherapy drugs was required to achieve a comparable reduction in cell viability of MDA-MB-231 cells seeded on silk-based matrices [84]. Moreover, a study that involved the co-culture of MDA-MB-231 cells with human osteoblast-like cells exhibited a greater viability when treated with the anti-cancer drug Paclitaxel compared to cancer cells cultured alone [82].

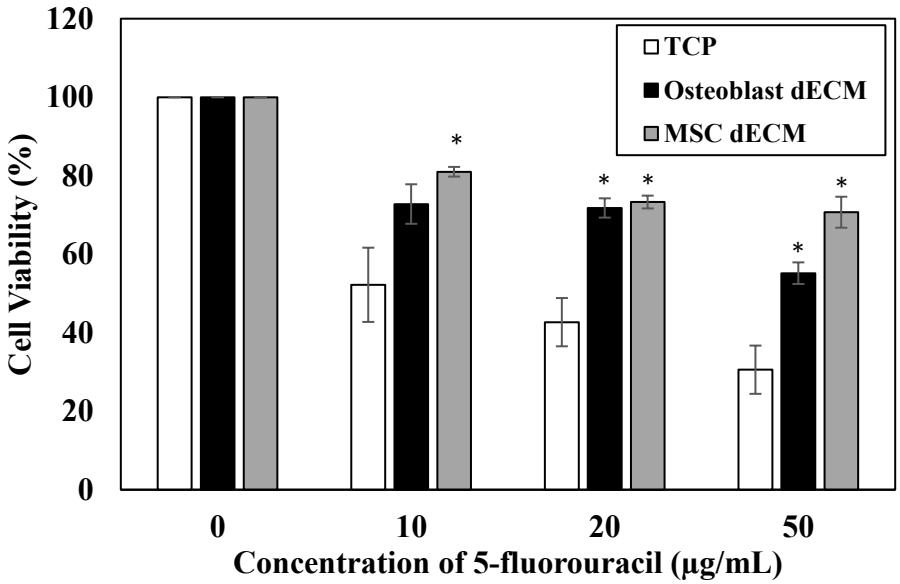

Figure 20. Effect of osteoblast- and MSC-derived ECM on the viability of MDA-MB-231 cancer cells after incubation with varying concentrations of chemotherapeutic agent, 5-fluorouracil. The viability was normalized with respect to cells incubated in similar environments with no drug. Error bar S.E.M (N=3). *p-value<0.05 with respect to cells cultured on TCP of the same drug concentration.

Chapter 11: Conclusion

In this study, mesenchymal stem cells (MSCs) were successfully differentiated into osteoblasts. Decellularized ECM from differentiated osteoblasts showed a greater deposition of collagen, fibronectin, and sulfated GAGs than MSC-derived matrices. The generated bone matrices were seeded with highly invasive breast cancer cells to study the effect of microenvironments on cancer cell behavior. Cancer cell proliferation increased when seeded on the bone matrices. Additionally, MDA-MB-231 cancer cells were challenged with 5-fluorouracil, a chemotherapeutic agent. Cells seeded on undifferentiated MSC- and differentiated MCS-derived matrices showed a significant reduction in the efficacy of the drug relative to cells seeded on wells with no matrices, suggesting an important role of the microenvironment, not only on cancer cell proliferation but on drug resistance properties as well.

Chapter 12: Future Studies

The work completed in part 1 of this thesis highlighted the role of matrix stiffness on the angiogenic activity of breast cancer cells through the release of angiogenesis-related factors. Future studies should include a 3D model of varying stiffness that houses both endothelial cells and cancer cells to study the direct effect of matrix compliance on the bioactivity of the released angiogenic factors. We predict that the endothelial cells would migrate towards the cancer cells in an attempt to form lumen-like structures due to the recruiting angiogenic signals released by the tumor cells. This model could potentially serve as an engineered tumor microenvironment that can be used in drug screening prior to drug testing trials on animals.

The second part of the thesis focused on creating a bone-like environment to better understand bone metastasis of breast cancer. The current work demonstrated that the osteogenic differentiation of MSCs resulted in the deposition of critical components of bone extracellular matrix. Further, it showed preliminary testing of generated dECM on the behavior of breast cancer cells. Taken together, the studies in parts 1 and 2 demonstrate that a matrix consisting of physiologically relevant properties, including both composition and stiffness, can be used to characterize the aggressive behavior of malignant breast cancer cells. Although this work is a step in the right direction, an *in-vitro* model is needed to capture the tumor cell-extracellular interaction. For this purpose, a bioprinted 3D bone metastasis model consisting of breast cancer cells and osteoblast-derived ECM as well as relevant variations in stiffness will be considered. Alginate, a naturally-derived polymer, is a suitable material to provide the structural support needed in this

model due to its low cost, biocompatibility, and ease of crosslinking as well as its widely used applications in tissue engineering and bioprinting, specifically.

References

1. Understanding Cancer. (2007). NIH Curriculum Supplement Series [Internet]. Retrieved from: https://www.ncbi.nlm.nih.gov/books/NBK20362/.

2. Shay, J., & Wright, W. (2000). Hayflick, his limit, and cellular ageing. *Nature Reviews Molecular Cell Biology, 1:* 72–76. doi:10.1038/35036093.

3. Weinberg, R.A. (1996). How cancer arises. *Scientific American. 275(3):*62-70. doi:10.1038/scientificamerican0996-62.

4. Zuazo-Gaztelu, I., & Casanovas, O. (2018). Unraveling the Role of Angiogenesis in Cancer Ecosystems. *Frontiers in Oncology. 8*. doi:10.3389/fonc.2018.00248.

5. Pittman, R.N. (2011). Regulation of Tissue Oxygenation. Chapter 2, The Circulatory System and Oxygen Transport.
   Retrieved from: https://www.ncbi.nlm.nih.gov/books/NBK54112/.

6. Patan S. (2004) Vasculogenesis and Angiogenesis. *In: Kirsch M., Black P.M. (eds)* Angiogenesis in Brain Tumors. *Cancer Treatment and Research, 117.* doi:10.1007/978-1-4419-8871-3_1.

7. Paku, S., & Paweletz, N. (1991). First steps of tumor-related angiogenesis. *Laboratory Investigation; a Journal of Technical Methods and Pathology. 65(3*):334-346.

8. Jain, R.K. (2003). Molecular regulation of vessel maturation. *Nature Medicine, 9:*685–93. doi:10.1038/nm0603-685.

9. Seyfried, T. N., & Huysentruyt, L. C. (2013). On the origin of cancer metastasis. *Critical Reviews in Oncogenesis, 18(1-2):* 43–73. doi:10.1615/critrevoncog.v18.i1-2.40.

10. Martin, T.A., Ye, L., Sanders, A.J., Lane, J., & Jiang, W.G. (2000-2013). Cancer Invasion and Metastasis: Molecular and Cellular Perspective. In: Madame Curie Bioscience Database [Internet]. Retrieved from: https://www.ncbi.nlm.nih.gov/books/NBK164700/.

11. Suva, L. J., Griffin, R. J., & Makhoul, I. (2009). Mechanisms of bone metastases of breast cancer. *Endocrine-related Cancer*, *16*(3): 703–713. doi:10.1677/ERC-09-0012.

12. Bendre, M., Gaddy, D., Nicholas, R.W., Suva, L.J. (2003). Breast cancer metastasis to bone: it is not all about PTHrP. *Clinical Orthopedics and Related Research.* S39–S45. doi:10.1097/01.blo.0000093844.72468.f4.

13. Acerbi, I., Cassereau, L., Dean, I., Shi, Q., Au, A., Park, C., Chen, Y. Y., Liphardt, J., Hwang, E. S., & Weaver, V. M. (2015). Human breast cancer invasion and aggression correlates with ECM stiffening and immune cell infiltration. *Integrative Biology, 7*(10): 1120–1134. doi:10.1039/c5ib00040h.

14. Handorf, A. M., Zhou, Y., Halanski, M. A., & Li, W. J. (2015). Tissue stiffness dictates development, homeostasis, and disease progression. *Organogenesis*, *11*(1): 1–15. doi:10.1080/15476278.2015.1019687.

15. Paszek, M.J., Zahir, N., Johnson, K.R., Lakins, J.N., Rozenberg, G.I., Gefen, A., ReinhartKing, C.A., Margulies, S.S., Dembo, M., Boettiger, D., Hammer, D.A., & Weaver, V.M. (2005). Tensional homeostasis and the malignant phenotype. *Cancer Cell, 8(3):*241-254. doi:10.1016/j.ccr.2005.08.010.

16. Jemal, A., Bray, F., Center, M.M., Ferlay, J., Ward, E., Forman, D. (2011). Global cancer statistics. *A Cancer Journal for Clinicians, 61:*69-90. doi: 10.3322/caac.20107.

17. Howlader, N., Noone, A.M., Krapcho, M., Miller, D., Brest, A., Yu, M., Ruhl, J., Tatalovich, Z., Mariotto, A., Lewis, D.R., Chen, H.S., Feuer, E.J., Cronin, K.A. (2018). SEER Cancer Statistics Review, 1975-2016, National Cancer Institute.

18. Carmeliet P, Jain RK. (2000). Angiogenesis in cancer and other diseases. *Nature, 407*:249-257. doi:10.1038/35025220.

19. Nishida, N., Yano, H., Nishida, T., Kamura, T., & Kojiro, M. (2006). Angiogenesis in cancer. *Vascular Health and Risk Management*, 2(3): 213–219. doi:10.2147/vhrm.2006.2.3.213.

20. Valastyan, S., & Weinberg, R.A. (2011). Tumor Metastasis: molecular insights and evolving paradigms. *Cell, 147:*275-292. doi:10.1016/j.cell.2011.09.024.

21. Hanahan, D., & Weinberg, R.A. (2000). The hallmarks of cancer. *Cell, 100 (1):*57–70. doi: 10.1016/s0092-8674(00)81683-9.

22. Lu, P., Weaver, V.M., & Werb, Z. (2012). The extracellular matrix: A dynamic niche in cancer progression. *The Journal of Cell Biology, 196 (4):* 395-406. doi:10.1083/jcb.201102147.

23. Hynes, R.O. (2009). The extracellular matrix: Not just pretty fibrils. *Science, 326:*1216–1219. doi:10.1126/science.1176009

24. Levental, K. R., Yu, H., Kass, L., Lakins, J. N., Egeblad, M., Erler, J. T., Fong, S., Csiszar, K., Giaccia, A., Weninger, W., Yamauchi, M., Gasser, D., & Weaver, V.M. (2009). Matrix crosslinking forces tumor progression by enhancing integrin signaling. *Cell, 139(5):* 891–906. doi:10.1016/j.cell.2009.10.027.

25. Egeblad, M., Rasch, M. G., & Weaver, V. M. (2010). Dynamic interplay between the collagen scaffold and tumor evolution. *Current Opinion in Cell Biology, 22(5):* 697–706. doi:10.1016/j.ceb.2010.08.015.

26. Boot-Handford, R.P., & Tuckwell, D.S. (2003). Fibrillar collagen: the key to vertebrate evolution? A tale of molecular incest. *Bioessays. 25 (2):*142-151. doi:10.1002/bies.10230.

27. Kalluri, R. (2003). Basement membranes: structure, assembly and role in tumour angiogenesis. *Nature Reviews Cancer, 3:*422–433. doi: 10.1038/nrc1094.

28. Pandya, P., Orgaz, J. L., & Sanz-Moreno, V. (2017). Actomyosin contractility and collective migration: may the force be with you. *Current Opinion in Cell Biology, 48:*87-96. doi:10.1016/j.ceb.2017.06.006.

29. Lo, C.M., Wang, H.B., Dembo, M., & Wang, Y.L. (2000). Cell movement is guided by the rigidity of the substrate. *Biophysical Journal, 79(1):*144–152. doi:10.1016/S0006-3495(00)76279-5.

30. Li, J., Wu, Y., Schimmel, N., Al-Ameen, M.A., & Ghosh, G. (2016). Breast cancer cells mechanosensing in engineered matrices: Correlation with aggressive phenotype. *Journal of the Mechanical Behavior of Biomedical Materials, 61*: 208-220. doi:10.1016/j.jmbbm.2016.01.021.

31. Dong, Y., Xie, X., Wang, Z., Hu, C., Zheng, Q., Wang, Y., Chen, R., Xue, T., Chen, J., Gao, D., Wu, W., Ren, Z., & Cui, J. (2014). Increasing matrix stiffness upregulates vascular endothelial growth factor expression in hepatocellular carcinoma cells mediated by integrin β1. *Biochemical and Biophysical Research Communications, 444(3):*427-432. doi:10.1016/j.bbrc.2014.01.079.

32. Chai, Q., Jiao, Y., & Yu, X. (2017). Hydrogels for Biomedical Applications: Their Characteristics and the Mechanisms behind Them. *Gels*, *3*(1): 6. doi:10.3390/gels3010006.

33. El-Sherbiny, I. M., & Yacoub, M. H. (2013). Hydrogel scaffolds for tissue engineering: Progress and challenges. *Global Cardiology Science & Practice*, *2013*(3): 316–342. doi:10.5339/gcsp.2013.38.

34. Roy, R., Boskey, A., & Bonassar, L. J. (2010). Processing of type I collagen gels using nonenzymatic glycation. *Journal of Biomedical Materials Research Part A*, *93*(3): 843–851. doi:10.1002/jbm.a.32231.

35. Mason, B.N., Starchenko, A., Williams, R.M., Bonassar, L.J., & Reinhart-King, C.A. (2013). Tuning three-dimensional collagen matrix stiffness independently of collagen concentration modulates endothelial cell behavior. *Acta Biomaterialia. 9(1):*4635–4644. doi:10.1016/j.actbio.2012.08.007.

36. Kass, L., Erler, J.T., Dembo, M., & Weaver, V.M. (2007). Mammary epithelial cell: Influence of extracellular matrix composition and organization during development and tumorigenesis. *The International Journal of Biochemistry & Cell Biology, 39 (11):*1987-1994. doi: 10.1016/j.biocel.2007.06.025.

37. De, S., Razorenova, O., McCabe, N.P., O'Toole, T., Qin, J., & Byzova, T.V. (2005). VEGF–integrin interplay controls tumor growth and vascularization. *Proceedings of the National Academy of Sciences, 102 (21):*7589-7594. doi:10.1073/pnas.0502935102.

38. Yu, H., Mouw, J.K., & Weaver, V.M. (2011). Forcing form and function: biomechanical regulation of tumor evolution. *Trends in Cell Biology, 21(1):*47–56. doi:10.1016/j.tcb.2010.08.015.

39. Samani, A., Bishop, J., Luginbuhl, C., & Plewes, D.B. (2003). Measuring the elastic modulus of ex vivo small tissue samples. *Physics in Medicine and Biology, 48*:2183-2189. doi:10.1088/0031-9155/48/14/310.

40. Lugano, R., Ramachandran, M. & Dimberg, A. (2019). Tumor angiogenesis: causes, consequences, challenges and opportunities. *Cellular and Molecular Life Sciences,* doi:10.1007/s000018-019-03351-7.

41. Apte, R.S., Chen, D.S., & Ferrara, N. (2019). VEGF in signaling and disease: beyond discovery and development. *Cell, 176(6):*1248–1264. doi:10.1016/j.cell.2019.01.021.

42. Hellstrom, M., Kalen, M., Lindahl, P., Abramsson, A., & Betsholtz, C. (1999). Role of PDGF-B and PDGFR-beta in recruitment of vascular smooth muscle cells and pericytes during embryonic blood vessel formation in the mouse. *Development, 126(14):*3047–3055.

43. Wilting, J., Birkenhager, R., Eichmann, A., Kurz, H., Martiny-Baron, G., Marme, D., McCarthy, J., Christ, B., & Weich, H.A. (1996). VEGF121 induces proliferation of vascular endothelial cells and expression of flk-1 without affecting lymphatic vessels of chorioallantoic membrane. *Developmental Biology, 176(1):*76–85. doi:10.1006/dbio.1996.9993.

44. Jiang, B.H., & Liu, L.Z. (2009). PI3 K/PTEN signaling in angiogenesis and tumorigenesis. *Advances in Cancer Research, 102*:19–65. doi: 10.1016/S0065-230X(09)02002-8.

45. van Hinsbergh, V.W., & Koolwijk, P. (2008). Endothelial sprouting and angiogenesis: matrix metalloproteinases in the lead. *Cardiovascular Research, 78(2):*203–212. doi:10.1093/cvr/cvm102.

46. Grose, R., & Dickson, C. (2005). Fibroblast growth factor signaling in tumorigenesis. *Cytokine & Growth Factor Reviews, 16 (2):*179-186. doi:10.1016/j.cytogfr.2005.01.003.

47. Miyake, M., Goodison, S., Lawton, A., Gomes-Giacoia, E., & Rosser, C. J. (2015). Angiogenin promotes tumoral growth and angiogenesis by regulating matrix metallopeptidase-2 expression via the ERK1/2 pathway. *Oncogene*, *34*(7): 890–901. doi:10.1038/onc.2014.2.

48. Dutta, D., Ghosh, S., Pandit, K., Mukhopadhyay, P., & Chowdhury, S. (2012). Leptin and cancer: Pathogenesis and modulation. *Indian Journal of Endocrinology and Metabolism*, *16*(Suppl 3): S596–S600. doi:10.4103/2230-8210.105577.

49. Artac, M., & Altundag, K. (2011). Leptin and breast cancer: An overview. *Medical Oncology, 29(3):*1510-1514. doi:10.1007/s12032-011-0056-0.

50. Doyle, S.L., Donohoe, C.L., Lysaght, J., & Reynolds, J.V. (2012). Visceral obesity, metabolic syndrome, insulin resistance and cancer. *Proceedings of the Nutrition Society, 71(1):*181–189. doi:10.1017/S002966511100320X.

51. Salomon, D.S., Normanno, N., Ciardiello, F., Brandt, R., Shoyab, M., & Todaro, G.J. (1995). The role of amphiregulin in breast cancer. *Breast Cancer Research and Treatment,* 33:103–114. doi:10.1007/BF00682718.

52. Cao, Y., & Xue, L. (2004). Angiostatin. *Seminars in Thrombosis and Hemostasis, 30(1):* 83-93. doi:10.1055/s-2004-822973.

53. Karpanen, T., Egeblad, M., Karkkainen, M.J., Kubo, H., Ylä-Herttuala, S., Jäättelä, M., & Alitalo, K. (2001). Vascular Endothelial Growth Factor C Promotes Tumor Lymphangiogenesis and Intralymphatic Tumor Growth. *Cancer Research, 61(5):* 1786-1790.

54. Ulrich, T.A., de Juan Pardo, E.M., & Kumar, S. (2009).The Mechanical Rigidity of the Extracellular Matrix Regulates the Structure, Motility, and Proliferation of Glioma Cells. *Cancer Research, 69(10):* 4167-4174. doi:10.1158/0008-5472.CAN-08-4859.

55. Suen, P.W., Ilic, D., Caveggion, E., Berton, G., Damsky, C.H., & Lowell, C.A. (1999). Impaired integrin-mediated signal transduction, altered cytoskeletal structure and reduced motility in Hck/Fgr deficient macrophages. *Journal of Cell Science, 112 (22)*: 4067–4078.

56. Ishizaki, T., Uehata, M., Tamechika, I., Keel, J., Nonomura, K., Maekawa, M., & Narumiya, S. (2000). Pharmacological properties of Y-27632, a specific inhibitor of Rho-associated kinases. *Molecular Pharmacology, 57(5*):976-983.

57. Kovacs, M., Toth, J., Hetenyi, C., Malnasi-Csizmadia, A., & Sellers, J. (2004). Mechanism of Blebbistatin Inhibition of Myosin II. *Journal of Biological Chemistry, 279:*35557-35563. doi:10.1074/jbc.M405319200.

58. Shoji, K., Oshashi, K., Sampei, K., Oikawa, M., & Mizuno, K. (2012) Cytochalasin D acts as an inhibitor of the actin-cofilin interaction. *Biochemical and Biophysical Research Communications, 424(1):* 52-57. doi:10.1016/j.bbrc.2012.06.063.

59. Fletcher, D. A., & Mullins, R. D. (2010). Cell mechanics and the cytoskeleton. *Nature*, *463*:485–492. doi:10.1038/nature08908.

60. Wang, A., Ma, X., Conti, M. A., & Adelstein, R. S. (2011). Distinct and redundant roles of the non-muscle myosin II isoforms and functional domains. *Biochemical Society Transactions*, *39(5*):1131–1135. doi:10.1042/BST0391131.

61. McGuire, A., Brown, J., A. L., & Michael, J. (2015). Metastatic breast cancer: the potential of miRNA for diagnosis and treatment monitoring. *Cancer and Metastasis Reviews, 34(1):*145-155. doi:10.1007/s10555-015-9551-7.

62. Macedo, F., Ladeira, K., Pinho, F., Saraiva, N., Bonito, N., Pinto, L., & Goncalves, F. (2017). Bone Metastases: an Overview. *Oncology Reviews*, *11*(1): 321. doi:10.4081/oncol.2017.321.

63. Barney, L. E., Dandley, E. C., Jansen, L. E., Reich, N. G., Mercurio, A. M., & Peyton, S. R. (2015). A cell-ECM screening method to predict breast cancer metastasis. *Integrative Biology, 7*(2): 198–212. doi:10.1039/c4ib00218k.

64. Sitarski, A. M., Fairfield, H., Falank, C., & Reagan, M. R. (2018). 3d Tissue Engineered In Vitro Models Of Cancer In Bone. *ACS biomaterials Science & Engineering, 4(2):*324–336. doi:10.1021/acsbiomaterials.7b00097.

65. Reichert, J.C., Quent, V.M., Burke, L.J., Stansfield, S.H., Clements, J.A., & Hutmacher, D.W. (2010). Mineralized human primary osteoblast matrices as a model system to analyse interactions of prostate cancer cells with the bone microenvironment. *Biomaterials, 31(31):*7928–36. doi:10.1016/j.biomaterials.2010.06.055.

66. Kolb, A. D., & Bussard, K. M. (2019). The Bone Extracellular Matrix as an Ideal Milieu for Cancer Cell Metastases. *Cancers*, *11*(7): 1020. doi.org/10.3390/cancers11071020.

67. Alford, A., Kozloff, K., & Hankenson, K. (2015). Extracellular matrix networks in bone remodeling. *International Journal of Biochemistry & Cell Biology, 65*:20–31. doi:10.1016/j.biocel.2015.05.008.

68. Raggatt, L.J., & Partridge, N.C. (2010). Cellular and Molecular Mechanisms of Bone Remodeling. *Journal of Biological Chemistry, 285:* 25103–25108. doi:10.1074/jbc.R109.041087.

69. Burstein, A.H., Zika, J.M., Heiple, K.G., & Klein, L. (1975). Contribution of collagen and mineral to the elastic-plastic properties of bone. *Journal of Bone and Joint Surgery, 57(7):*956–961. doi:10.2106/00004623-197557070-00013.

70. Alberts, B., Johnson, A., Lewis, J., Raff, M., Roberts, K., & Walter, P. (2015). Molecular Biology of the Cell. 6th ed. American Society for Cell Biology; New York, NY, USA: 2015.

71. Matsugaki, A., Aramoto, G., Ninomiya, T., Sawada, H., Hata, S., & Nakano, T. (2015). Abnormal arrangement of a collagen/apatite extracellular matrix orthogonal to osteoblast alignment is constructed by a nanoscale periodic surface structure. *Biomaterials, 37*:134–143. doi:10.1016/j.biomaterials.2014.10.025.

72. Wang, J., Jia, F., Gilbert, T., & Woo, S. (2003). Cell orientation determines the alignment of cell-produced collagenous matrix. *Journal of Biomechanics*, *36 (1)*:97–102. doi:10.1016/S0021-9290(02)00233-6.

73. Shi, S., Kirk, M., & Kahn, A.J. (1996). The role of type I collagen in the regulation of the osteoblast phenotype. *Journal of Bone and Mineral Research, 11(8):*1139–1145. doi: 10.1002/jbmr.5650110813.

74. Fernandes, H., Mentink, A., Bank, R., Stoop, R., van Blitterswijk, C., & de Boer, J. (2010). Endogenous collagen influences differentiation of human multipotent mesenchymal stromal cells. *Tissue Engineering Part A, 16(5):*1693–1702. doi:10.1089/ten.tea.2009.0341.

75. Pankov R., Yamada K.M. (2002). Fibronectin at a glance. *Journal of Cell Science, 115(20):*3861–3863. doi: 10.1242/jcs.00059.

76. Globus, R., Doty S., Lull, J., Holmuhamedov, E., Humphries, M., & Damsky C. (1998). Fibronectin is a survival factor for differentiated osteoblasts. *Journal of Cell Science, 111(10)*:1385–1393.

77. Mansouri, R., Jouan, Y., Hay, E., Bin-Wakkach, C., Frain, M., Ostertag, A., Henaff, C., Marty, C., Geoffroy, V., Marie, P.J., Cohen-Solal, M., & Modrowski, D. (2017). Osteoblastic heparan sulfate glycosaminoglycans control bone remodeling by regulating Wnt signaling and the crosstalk between bone surface and marrow cells. *Cell Death & Disease, 8*, e2902. doi:10.1038/cddis.2017.287.

78. Sears, V., & Ghosh, G. (2020). Harnessing mesenchymal stem cell secretome: Effect of extracellular matrices on proangiogenic signaling. *Biotechnology and Bioengineering, 117 (4):*1159– 1171. doi:10.1002/bit.27272.

79. Stenman, S., & Vaheri, A. (1981). Fibronectin in human solid tumors. *International Journal of Cancer. 27(4):*427–435. doi:10.1002/ijc.2910270403.

80. Wang, K., Wu, F., Seo, B.R., Fischbach, C., Chen, W., Hsu, L., & Gourdon, D. (2017). Breast cancer cells alter the dynamics of stromal fibronectin-collagen interactions. *Matrix Biology, 60–61:*86–95. doi: 10.1016/j.matbio.2016.08.001.

81. Ye, M., Mohanty, P., & Ghosh, G. (2014). Biomimetic apatite-coated porous PVA scaffolds promote the growth of breast cancer cells. *Materials Science and Engineering:C, 44:* 310 - 316. doi: 10.1016/j.msec.2014.08.044.

82. Talukdar, S. and Kundu, S.C. (2013), Engineered 3D Silk-Based Metastasis Models: Interactions Between Human Breast Adenocarcinoma, Mesenchymal Stem Cells and Osteoblast-Like Cells. *Advanced Functional Materials, 23 (42):* 5249-5260. doi:10.1002/adfm.201300312.

83. Pathi, S. P., Lin, D. D., Dorvee, J. R., Estroff, L. A., & Fischbach, C. (2011). Hydroxyapatite nanoparticle-containing scaffolds for the study of breast cancer bone metastasis. *Biomaterials*, *32(22*): 5112–5122. doi.org/10.1016/j.biomaterials.2011.03.055.

84. Talukdar, S., & Kundu, S.C. (2012), A Non-Mulberry Silk Fibroin Protein Based 3D In Vitro Tumor Model for Evaluation of Anticancer Drug Activity. *Advanced Functional Materials, 22 (22):* 4778-4788. doi:10.1002/adfm.201200375.